ESA O_3-CCI Project (Phase 3)

Climate Assessment Report (CAR)

by Martin Dameris[1], Melanie Coldewey-Egbers[2], and Michiel van Weele[3]

[1] Deutsches Zentrum für Luft- und Raumfahrt, Institut für Physik der Atmosphäre, Oberpfaffenhofen, Germany

[2] Deutsches Zentrum für Luft- und Raumfahrt, Institut für Methodik der Fernerkundung, Oberpfaffenhofen, Germany

[3] Koninklijk Nederlands Meteorologisch Instituut, De Bilt, Netherlands

This climate assessment report builds on the two previous climate assessment reports, which were prepared in 2014 and 2017 in the context of the ESA Ozone_cci project. New insights and recent results of data analyses and numerical modelling of the atmosphere, in particular with respect to stratospheric ozone, have been added.

1. Introduction, purpose and scope of the CAR

Europe has the responsibility to perform long-term measurements of Essential Climate Variables (ECVs) and to evaluate and investigate the ECVs, to meet obligations regarding the monitoring of international agreements, in particular the protocols of Montreal and Kyoto. Therefore, it is one of the highest priority tasks for European and national agencies (e.g. ESA, research funders) and the scientific community to work on the creation and maintenance of ECV records. The implementation of appropriate missions and programs are technically and scientifically challenging. It is becoming increasingly clear that monitoring of atmospheric composition and other relevant climate variables is essential, to detect and enable investigations of short- and long-term variations including possible trends, and to provide a better understanding of atmospheric mechanisms driving the climate system. This is absolute essential aiming to enhance the scientific knowledge of the relevant physical, dynamical and chemical processes in Earth atmosphere and gaining deeper insights of their interactions. For example, it is necessary to investigate in detail specific physical, chemical and dynamical processes of the atmosphere including their interactions, especially the chemistry-climate feedback mechanisms. In this respect, process-oriented studies using numerical modelling support such scientific investigations. In the context with the analyses of high-quality data sets derived from observations, they help to identify weaknesses of our atmospheric models and to correct adequately the description of atmospheric behavior. This is also the most important foundation for an evaluation of past and present changes of atmospheric conditions and enables robust predictions of climate change and modifications of the chemical composition of the atmosphere. For instance, the expected recovery of the stratospheric ozone layer in the next decades in the light of climate change has to be checked and investigated. In addition, the accompanying investigation and analysis of the long-term observations and numerical modelling was become clear particularly in recent years: The detected,

unexpected strong emissions of CFC-11 (Montzka et al., 2018; 2021; WMO, 2021) raised immediately questions with respect to possible consequences for the ozone layer. Based on numerical simulations with chemistry-climate models specific answers were given and clear statements and assessments were received (Dameris et al., 2019; Fleming et al., 2020; Keeble et al., 2020; see Section 2). The evolution of the stratospheric ozone layer considering the evolution of tropospheric ozone in a future climate must be further studied. It is expected that there will be significant regional differences regarding the timing of the recovery (or return to 1980-levels) of the ozone layer.

Comprehensive global long-term data sets of ECVs with high quality standards are required to provide the foundation for a complete description of the current status of Earth climate and the evolution in the recent decades, in particular allowing an adequate reproduction of the Earth climate system with our numerical model systems. One important task of atmospheric models is to project future evolution of climate change and possible risks. In the face of outstanding great challenges regarding effects of climate change and modifications of our environment, mitigation and adaptation strategies have to be investigated using a robust database. Therefore, necessary requirements for ECV data sets are long-term stability, precision, characterization of errors, and continuity. Science strongly needs further continuation of observations, i.e. monitoring of ECVs, to detect as quick as possible important changes of the Earth climate system. It is not only necessary to perform measurements, but also to provide high quality derived data products (from Level 0 to Level 3+) that permit respective scientific examinations. We definitely need long-term measurements to identify clear trends in a statistic manner.

ESA-CCI has enabled ESA and European scientists to contribute significantly to coordinated international actions on climate observations from space. European scientists play vital parts in international climate research programs (such as WCRP) and in recent international assessment reports, in particular ESA-CCI has made valuable contributions to IPCC's 5th and 6th Climate Assessment reports, the most recent UNEP/WMO Scientific Assessment of Ozone Depletion published in 2014 and 2018, and other important high-ranking final documents like the SPARC project LOTUS (Long-term Ozone Trends and Uncertainties in the Stratosphere; SPARC/IO3C/GAW, 2019), or the Tropospheric Ozone Assessment Report (TOAR; Tarasick et al., 2019). The ESA-CCI has helped to increase the visibility of European research and researchers in this specific field.

As already mentioned before, such an ECV database is crucially important, supporting the goals of protecting Earth climate and the environment in the international context. In this context, the ECV "ozone" is one of the most important climate agents. It is well known that the stratospheric ozone layer protects the Earth surface from ultra-violet radiation. Beyond that the extreme ozone loss over Antarctica in spring has obviously changed surface climate significantly (see Chapter 4 in WMO, 2014; Banerjee et al., 2020). Clear indications were also presented of

connections of Arctic stratospheric ozone extremes to Northern Hemisphere surface climate (e.g. Ivy et al., 2017).

The generation of homogeneous, high-quality long-term (multi-year/-decadal) data sets, which allow the investigation of relevant processes and how processes are changing in space and time are still needed. Recent data sets have to be combined together in a consistent manner to enable a uniform picture of recent fluctuations and changes. This is one prerequisite to add new future measurements allowing identification and investigation of short- and long-term fluctuations and trends. A nice example is the combination of total ozone values derived from the Tropospheric Monitoring Instrument (TROPOMI) sensor on board the Sentinel-5 Precursor satellite with the long-term ozone data set from the European satellite data record GOME-type Total Ozone Essential Climate Variable (GTO-ECV) from July 1995 to June 2019 (Coldewey-Egbers et al., 2015; Dameris et al., 2021).Scientists need high-quality data sets to support excellent scientific investigations of atmospheric fluctuations and changes and of the processes involved. The usefulness of the data products has to be demonstrated by helping to answer climatically relevant questions. In particular in the Ozone_cci project substantial community building has taken place to strengthen the relationship between satellite data product developers and climate scientists. Ozone_cci has produced long, consistent time series (currently 1995-2020 including TROPOMI data) of total ozone column and ozone vertical profile measurements from multiple nadir and limb sounding instruments. Consistency between these European data sets and other ozone data products (derived from US instruments, e.g., TOMS, SBUV, OMPS, HALOE, SAGE, MLS) has been investigated (future plan: merged data sets, to extend the length of the data series). Some of these results are discussed in the following.

2. Scientific tasks and current investigations

Consistent, multi-year data sets are needed for scientific research. In particular for the ECV ozone there are some outstanding questions, which must be investigated in the coming years. There is need for extending the CCI scientific program and to continue with the monitoring of the stratospheric ozone layer. An outstanding example was the detection of unexpected emissions of CFC-11 (Montzka et al., 2018), the identification of their causes (Rigby et al., 2019), the immediate scientific reviewing of consequences for the ozone layer (Dameris et al., 2019; Dhomse et al., 2019; Fleming et al., 2020; Keeble et al., 2020), and the quick reaction of the responsible actors, which was documented again by observations (Montzka et al., 2021; WMO, 2021). Available long-term data sets (e.g. multi-decadal observations of total ozone column; see the recent WMO Scientific Assessments of Ozone Depletion, 2007, 2011, 2014, and 2018) have demonstrated impressively their usefulness; it is obvious that a continuation of these data series is required.

Regarding ozone, the current scientific challenges, questions and tasks are:

- Continuous monitoring of the consequences of the Montreal Protocol and its amendments, in particular the
- detection of ozone return/recovery in the next 5 to 10 years, i.e., identifying the reversal point in time where stratospheric ozone decline stalls due to the regulation of CFCs and the ozone layer will start to recover. It has to be investigated if the recovery of ozone in the upper stratosphere is consistent with our expectations based on Cl_y (e.g., WMO, 2021), temperature (e.g., Maycock et al., 2018), and other factors; and
- further monitoring of the ozone layer change over the 21st century (including in respect of atmospheric changes from sudden stratospheric warmings, the accelerated Brewer Dobson circulation as a consequence of climate change, or possibly enhanced interannual dynamically induced fluctuations, etc.) is necessary, in particular detecting higher stratospheric ozone values as an indicator of climate change (e.g., Dhomse et al., 2018; Keeble et al., 2021).
- Multi-year comprehensive 4D-ozone data bases are the foundation for understanding of dynamical and chemical processes and their feedback (coupling) affecting the ozone layer.
- Comprehensive data bases are needed to check the abilities of Chemistry-Climate Models (CCMs) to reproduce observed features and short- and long-term variability.
- CCM simulations are used to predict the future evolution of the stratospheric ozone layer in a changing climate, determining the dependence of ozone recovery in space (latitude and altitude) and time, especially investigating the evolution of the ozone layer in polar regions (ozone hole) as well as the tropics and its impact on surface climate.

- How important is climate change for the future evolution of the tropospheric ozone (e.g. Stratosphere-Troposphere Exchange, STE)? How will ozone concentrations develop in the troposphere depending on the assumed climate scenarios and the expected emissions of ozone precursors? I.e., examination of the importance of STE processes for tropospheric ozone and the impact of climate change on STE; what is expected for the future? How strong will they affect the total ozone column?
- Investigation of the importance of increasing tropospheric ozone as a hemispheric pollutant and climate forcer related to ozone precursor emissions.
- Working on the importance of (changes in) troposphere-stratosphere transport, for instance in the Asian monsoon region for the evolution of the ozone layer (e.g., Adcock et al., 2021).
- Examination of the importance of ozone-radiative and ozone-dynamical interactions in the lower stratosphere and the impact of climate change on these interactions.
- And, last but not least making an attempt getting boundary layer ozone and mid-upper tropospheric ozone concentration distributions and trends worldwide (probably best achieved through reanalysis that uses the full integrated observing system).

3. Examples of new ozone analyses and current status of knowledge

In this section a short review of recent and ongoing scientific work regarding atmospheric ozone are presented, in particular, those related to this climate assessment report. The Ozone_cci Climate Research Group is working on a number of aspects. Examples are given in the following.

3.1 Highlights of the recent WMO ozone assessment and open question

Every four years, the current status of knowledge regarding the evolution of the stratospheric ozone layer is summarized in a scientific report, which is organized by UNEP and WMO. In the following, some of the most outstanding statements presented in the last UNEP/WMO Scientific Assessment of Ozone Depletion (2018 are briefly summarized:

- The atmospheric abundances of both total tropospheric chlorine and total tropospheric bromine from long-lived ozone depleting substances (ODSs) controlled under the Montreal Protocol have continued to decline since the 2014 Ozone Assessment.
- Global CFC-11 emissions increased after 2012 contrary to projections from previous Ozone Assessments, which showed decreasing emissions (Montzka et al., 2018). [See the later publications of Montzka et al. (2021) and WMO (2021) indicating a significant decline of CFC-11 emissions in 2018 and 2019.]
- Total chlorine (bromine) entering the stratosphere from well-mixed ODSs declined by 12% (15%) between the 1993 (1998) peak value and 2016.
- For the first time, there are emerging indications that the Antarctic ozone hole has diminished in size and depth since the year 2000, with the clearest changes occurring during early spring. Although accounting for natural variability is challenging, the weight of evidence suggests that the decline in ODSs made a substantial contribution to the observed trends.
- Even with these early signs of recovery, an Antarctic ozone hole continues to occur every year, with the severity of the chemical loss strongly modulated by meteorological conditions. [See for instance the situation observed in 2020, https://www.esa.int/Applications/Observing_the_Earth/Copernicus/Sentinel-5P/Antarctic_ozone_hole_is_one_of_the_largest_and_deepest_in_recent_years, “Antarctic ozone hole is one of the largest and deepest in recent years”.]
- In the Arctic, year-to-year variability in column ozone is much larger than in the Antarctic, precluding identification of a statistically significant increase in Arctic ozone over the 2000-2016 period. [See also e.g. Dameris et al., 2021.]
- Model simulations show that implementation of the Montreal Protocol has prevented much more severe ozone depletion than has been observed in the polar regions of both hemispheres.

- No statistically significant trend has been detected in global (60°S-60°N) total column ozone over the 1997-2016 period. Upper stratospheric ozone has increased by 1-3% per decade since 2000 outside of polar regions.
- There is some evidence for a decrease in global (60°S-60°N) lower stratospheric ozone from 2000 to 2016, but it is not statistically significant in most analyses. Much of the apparent decline in the tropics and mid-latitudes was reversed by an abrupt increase in ozone in 2017, showing that longer records are needed to identify robust trends.
- Based on CCM scenario simulation results, the Antarctic ozone hole is expected to gradually close, with springtime total column ozone returning to 1980 values shortly after mid-century (about 2060). Arctic springtime total ozone is expected to return to 1980 values before mid-century (about 2030s). Northern-Hemisphere mid-latitude column ozone is expected to return to 1980 abundances before mid-century (2030s), and Southern Hemisphere mid-latitude ozone is expected to return around mid-century.
- Outside the Antarctic, carbon dioxide (CO_2), methane (CH_4), and nitrous oxide (N_2O) will be the main drivers of stratospheric ozone changes in the second half of the 21st century, assuming full compliance with the Montreal Protocol. [See update in Keeble et al. (2021).]
- Discrepancies between estimates of stratospheric cooling rates from different satellite temperature retrievals have been substantially reduced since the last Ozone Assessment (see Maycock et al., 2018). Decreases in stratospheric ozone caused by ODS increases have been an important contributor to observed stratospheric cooling. Satellite temperature records show weaker global-average cooling throughout the depth of the stratosphere between 1998 and 2016 relative to between 1979 and 1997.
- New studies strengthen the conclusion from the last Ozone Assessment that lower stratospheric cooling due to ozone depletion has very likely been the dominant cause of late 20th century changes in Southern Hemisphere climate in summer. Changes in tropospheric circulation driven by ozone depletion have contributed to recent trends in Southern Ocean temperature and circulation.

More detailed descriptions and explanations are discussed in the following with respect to the future evolution of the global and polar ozone layer and how it is connected with climate change.

Ozone-depleting substances (ODSs) were the dominant driver of global ozone decline in the late 20th century. It is now very clear that as controlled ODS concentrations decline, CO_2, N_2O, and CH_4 will strongly influence ozone evolution in the latter part of the 21st century through chemical and climate effects. Uncertainties

in future emissions of these gases lead to large differences in ozone projections at the end of the century (Dhomse et al., 2018; WMO, 2018; Keeble et al., 2021).

It is evident that climate change is not only affecting the troposphere (enhanced greenhouse gases leads to a warming) but is also modifying the stratosphere (leading to a cooling). In this connection important questions are:

(i) How are the interactions between climate change and modifications of the circulation and chemical composition of the stratosphere?

(ii) How is climate change influencing the stratospheric ozone layer?

Due to lower stratospheric temperatures, ozone chemistry is directly affected. For example, the content of ozone (O_3) in the middle and upper stratosphere is globally enhanced due to reduced ozone depletion by slower homogeneous gas phase reactions, while in the polar lower stratosphere the enhanced probability of polar stratospheric clouds intensifies ozone depletion.

As controlled ODSs decline, the evolution of the ozone layer in the second half of the 21st century will largely depend on the atmospheric abundances of greenhouse gases. Overall, increasing CO_2 and CH_4 elevate global ozone while increasing N_2O further depletes global ozone (**Figure 1**).

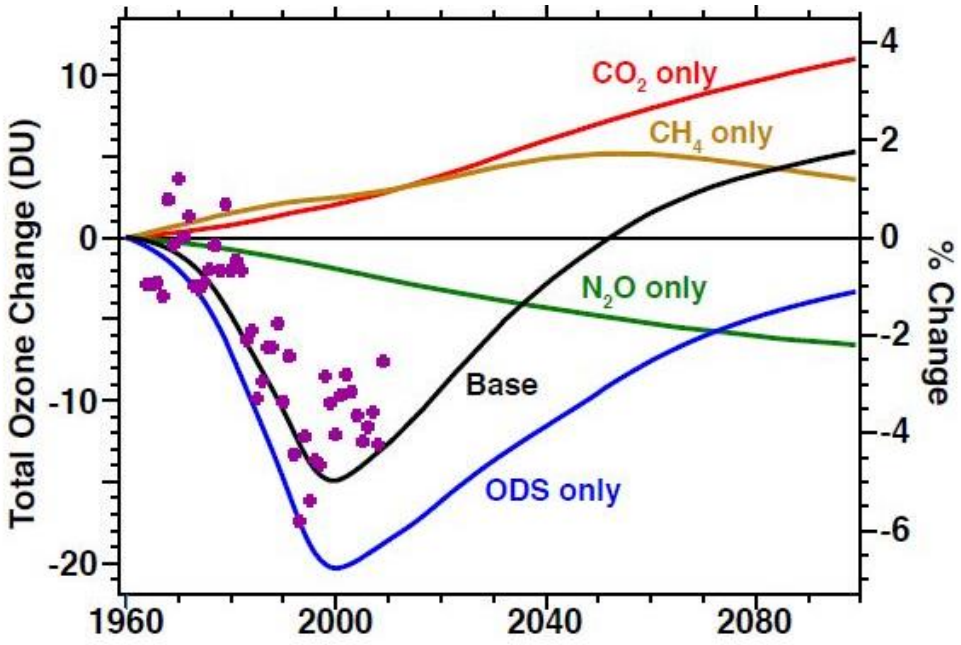

Figure 1: Sketch of model-simulated global and annual averaged total ozone response to the changes in CO_2 (red line), CH_4 (brown line), N_2O (green line), and ODSs (blue line). The total response to ODSs and greenhouse gases combined is shown as the black line. The responses are taken relative to 1960 values. Ground-based total ozone observations (base-lined to the mid-1960s) are shown as magenta cross symbols (the figure is taken from WMO, 2014).

Total column ozone is projected during the 21st century in more detail on the foundation of multi-model-means (MMM) of CCM simulation results, under the presumption of different climate scenario (**Figure 2**). There are several indications that the ozone layer is beginning to recover from ODS-induced depletion.

Tropical ozone levels are only weakly affected by the decline of ODSs. They are sensitive to circulation changes (i.e. a stronger upwelling of tropical air masses) driven by CO_2, N_2O, and CH_4 increases. As a result, in the tropics decreases in total column ozone are calculated, depending on the prescribed climate scenario. Tropical ozone changes in future will be definitely dominated by enhanced greenhouse gas concentrations (e.g., Dhomse et al., 2018; Meul et al., 2016).

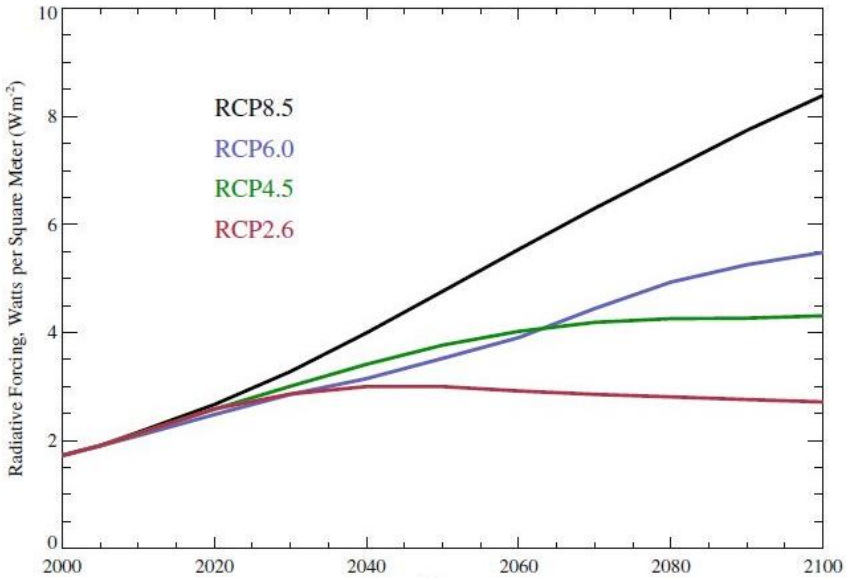

Figure 2: Boundary conditions for the different climate scenarios, i.e. the representative concentration pathway (RCP), as defined for the climate model scenario simulations.

The projected future evolution of tropical total column ozone is strongly dependent on future abundances of CO_2, N_2O, and CH_4 (e.g., as in Representative Concentration Pathways (RCPs)), and is particularly sensitive to changes in the tropical upwelling and changes in tropospheric ozone. In particular for RCP4.5, which specifies weaker increases in greenhouse gas concentrations (compared to RCP6.0 or RCP8.5), significant decreases in total column ozone are projected during the 21st century (**Figure 3**). An explanation is that in the case of the RCP4.5 scenario the increase of upper stratosphere ozone (due to reduced stratospheric temperatures) is clearly compensated by enhanced upwelling (of tropospheric air masses with reduced ozone concentrations, leading to a significant reduction of lower stratospheric ozone). See below the further discussion of results.

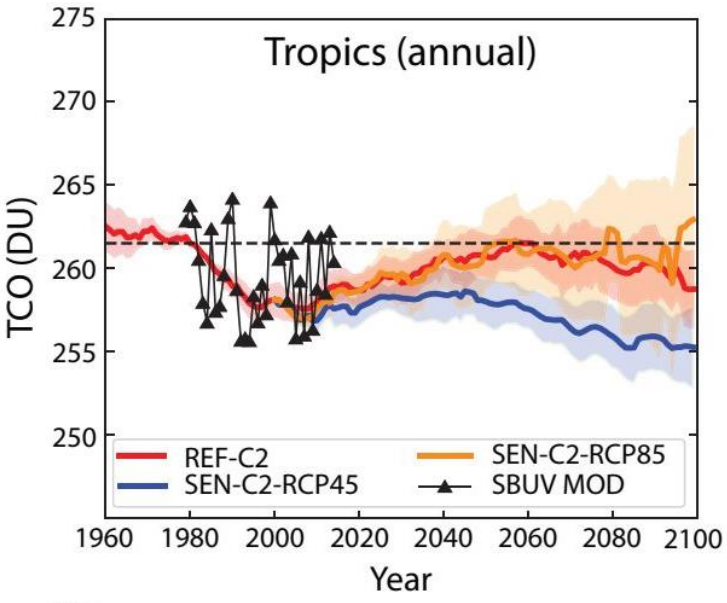

Figure 3: Total column ozone time-series averaged over the tropical latitude band 25°S-25°N derived from Chemistry-Climate Model simulations for three RCP scenarios RCP4.5 (i.e. the sensitivity simulation SEN-C2-RCP45), RCP6.0 (i.e. the simulation REF-C2), and RCP8.5 (i.e. SEN-C2-RCP85). The thick color lines are showing the mean of all models (MMM). Also shown are total column ozone values derived from satellite observations (SBUV, black triangles) (figure taken from Dhomse et al., 2018).

The future evolution of the polar ozone layer shows differences with regard to the Arctic and Antarctic stratosphere (**Figure 4**). The Antarctic ozone hole will continue to occur at least until mid-century. Occasional large Arctic ozone depletion, such as that in spring 2011, is well understood, and is also possible in coming decades. Such an event was observed again in spring 2020 (e.g., Dameris et al., 2021), showing record low ozone values over the Arctic. Recovery of polar ozone would occur earlier if there were no further emissions of controlled ODSs, and would be delayed by increases in stratospheric aerosol content that could be caused by injection of sulfur by large volcanic eruptions or by man-made activities affecting stratospheric ozone depleting chemistry, for instance by enhanced nitrous oxide (N_2O) emissions (Ravishankara et al., 2009), as indicated in **Figure 1**.

There are clear indications that stratospheric changes, in particular changes related to ozone depletion, have an effect on surface weather and climate. It has been shown that the Antarctic ozone hole has caused significant changes in Southern Hemisphere surface climate, e.g. the summertime tropospheric circulation has been affected in the recent decades, with associated impacts on surface conditions (e.g., Thompson et al., 2011; Barnes et al., 2019; Banerjee et al., 2020).

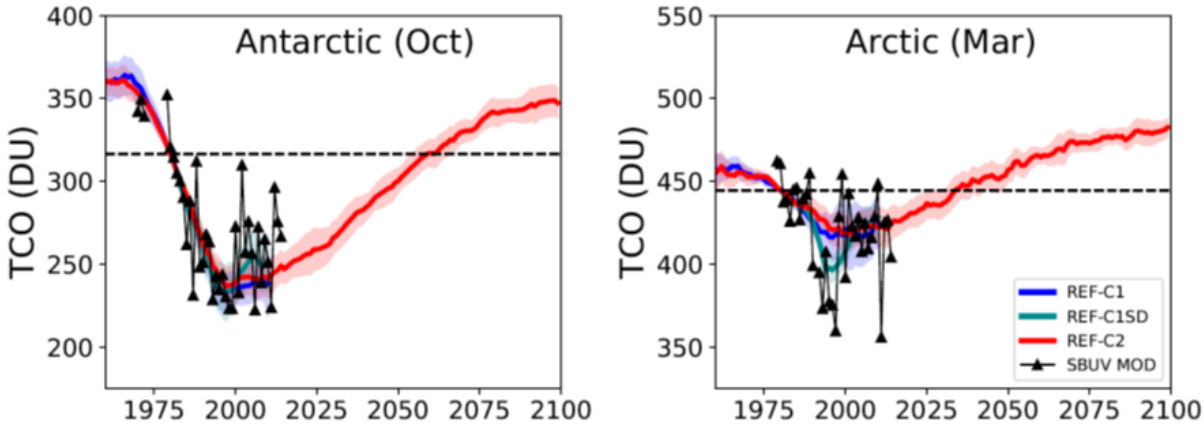

***Figure 4**:* Total column ozone time-series averaged over the polar regions in spring derived from Chemistry-Climate Model (CCM) simulations. The multi-model-mean (MMM) is only presented for the REF-C2 (in red, i.e. RCP6.0). The blue and green line indicate results of CCM simulations representing the past. The black triangles are showing satellite observations (SBUV).

3.2 Comparison of Ozone_cci total columns with CCM simulations

Validation of model results derived from CCM simulations[1] for the past with ozone data derived from European space-borne-instruments have been carried out. The performance of such ozone data sets are analysed and results of supporting modelling efforts with CCMs are confronted with Ozone-cci data products. The synergies of model data and observations are exploited to address scientific questions, e.g., assessment of ozone depletion and recovery in a changing climate, interannual variability and extremes and regional changes of the ozone distribution.

Ozone data products derived from long-term (multi-year) CCM simulations (e.g., 1980 to 2017) are provided. Among others using set ups of the CCM with specified dynamics (in the so-called “nudged mode” using a relaxation towards observed dynamic fields) to be able to compare with specific observations. The CCMs mostly include a comprehensive description of stratospheric ozone chemistry (a complete overview of the used CCMs is presented by Morgenstern et al., 2017).

For instance, two simulations performed with version 2.51 of the European Centre for Medium-Range Weather Forecasts – Hamburg (ECHAM) / Modular Earth Submodel System (MESSy) Atmospheric Chemistry (EMAC) model have been confronted with the ESA Ozone_cci GOME-type Total Ozone Essential Climate Variable (GTO-ECV) data record (Coldewey-Egbers et al., 2015). A detailed description of the model system and its different set-ups can be found in Jöckel et al. (2016) and references therein. We investigated two hindcast simulations (1980-2013) with specified dynamics, i.e. meteorology nudged towards ERA-Interim reanalysis data (Dee et al.,

[1] The CCM simulations were defined on the basis of the SPARC/IGAC Chemistry-Climate Model Initiative (CCMI), in particular to support the WMO Scientific Assessment of Ozone Depletion: 2018 (see http://www.geo.fu-berlin.de/met/ag/strat/publikationen/docs/Eyring-et-al_SPARC-Newsletter40.pdf).

2011). The nudging is applied for the prognostic variables divergence, vorticity, temperature, and surface pressure, in which the nudging strength varies with altitude. Sea surface temperatures and sea ice concentrations are taken from ERA-Interim reanalysis data, too. The so-called “RC1SD-base-07” simulation includes the nudging of the global mean temperature, whereas this is omitted in the second simulation “RC1SD-base-10”.

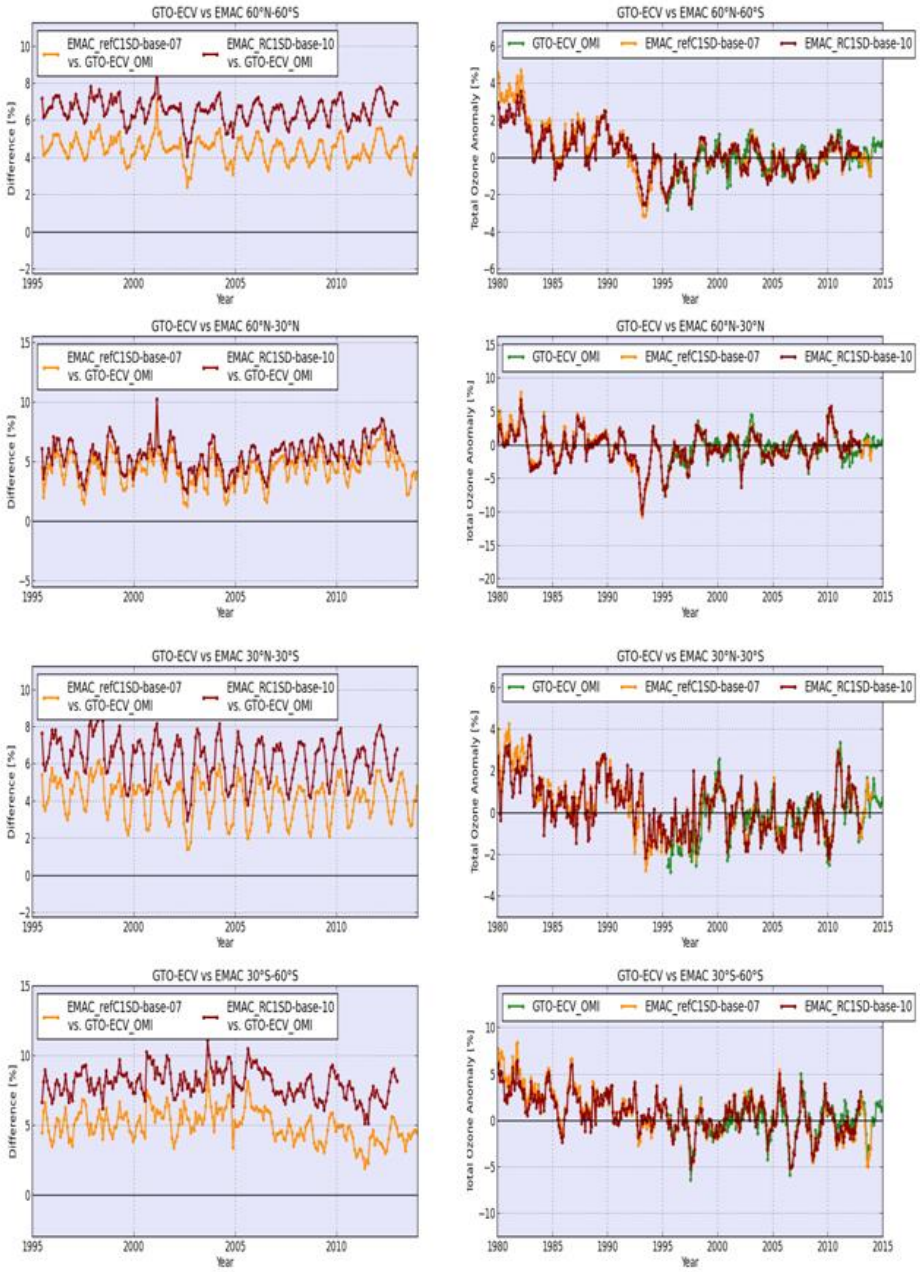

Figure 5: Left column: Difference [%] as a function of time from 1995 to 2013 between EMAC model simulations and GTO-ECV total ozone data. Right column: Total ozone anomalies [%] from 1980 to 2015. From top to bottom: Latitude belts 60°N-60°S, 60°N-30°S, 30°N-30°S, and 30°S-60°S. Red: RC1SD-base-10 simulation, yellow: RC1SD-base-07 simulation and green: GTO-ECV satellite data.

Jöckel et al. (2016) provided a first evaluation of the modeled ozone distributions by comparing with observations such as satellite measurements and ozone sonde data. They found that total ozone columns are overestimated for all latitude bands with the bias generally increasing from north to south. The simulation RC1SD-base-07 with temperature nudging agrees better with the observations than the corresponding simulation without nudging the global mean temperature.

Figure 5 shows the monthly mean differences between model simulations and GTO-ECV data (left) and ozone anomalies for simulations and GTO-ECV (right) as a function of time for different latitude bands: 60°N-60°S, 60°N-30°N, 30°N-30°S, and 30°S-60°S, from top to bottom. Anomalies have been calculated with respect to the multi-year average from 1998 to 2012.

Total ozone is slightly overestimated for both simulations. The bias is larger in the Southern Hemisphere than in the Northern Hemisphere. Nudging the global mean temperature (RC1SD-base-07, yellow curves) reduces the bias between model and observation, in particular in the tropics and the middle latitudes of the Southern Hemisphere. The reduction in the Northern Hemisphere is smaller, because the bias is reduced only in the troposphere, whereas in the stratosphere it is enlarged (Jöckel et al., 2016).

Ozone anomalies (**Figure 5**, right column) show an excellent agreement between simulations (both nudging versions, yellow and red curves) and observations (green curves). During the overlap period, interannual variability is very well captured by the model system, and extreme values are well reproduced in most cases.

Figure 6 shows the same as **Figure 5**, but for March values in the northern high latitudes (85°N-60°N, top row) and for October values in the southern high latitudes (60°S-85°S, bottom panels). As for the other latitude bands (**Figure 5**) the model has a positive bias for total ozone columns in both polar regions (left column). The bias is significantly reduced when the nudging includes the global mean temperature (RC1SD-base-07, yellow curve). Furthermore, the model is able to capture ozone anomalies even in high latitudes (right column) and in extreme cases such as the record low ozone values in the Arctic in March 1997 and 2011 and in October 2002 when the Antarctic polar stratospheric vortex was disturbed and split up into two parts.

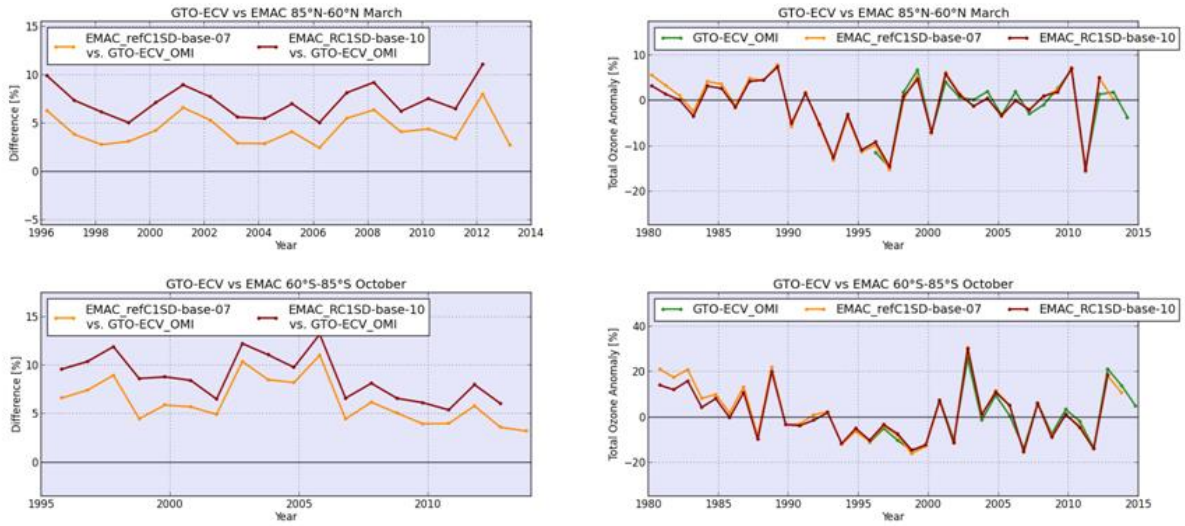

Figure 6: Top row: Relative difference [in %] from 1995-2013 between EMAC model simulation and GTO-ECV total ozone column (left) and ozone anomalies [in %] from 1980-2015 for EMAC and GTO-ECV for March, 85°N-60°N. Bottom panels: same as top panels, but for October, 60°S-85°S.

The combination of CCM data based on simulations with specified dynamics allows determining the recent evolution of the ozone layer in a consistent manner. Since the ozone anomalies calculated from the CCM are in excellent agreement with the respective Ozone_cci data product, reliable signs for the temporal development of the ozone layer in specific regions can be identified. For instance, in **Figures 5 and 6** obvious reduction of the total ozone amount is detected, but with different amplitudes: In the northern mid-latitudes there is no statistically significant trend over the last 35 years (Figure 5, right column, second row), whereas the southern mid-latitudes show a clear reduction of the ozone content by about 5% until the year 1997 (Figure 5, right column, forth row). In the tropics (Figure 5, right column, third row) the ozone reduction before 1995 is in the order of 2-3%. The anomalies show a clear signature of the 11-year solar cycle, as discussed in detail in the WMO ozone report of 2006 (WMO, 2007). During spring time, both polar regions indicate a strong trend of ozone depletion, i.e. about 15% in the Arctic stratosphere and up to 35% in the Antarctic stratosphere, which are stopped around 1997 (Figure 6, right column). So far, no latitudinal region of the stratosphere is showing an obvious beginning of ozone recovery.

3.3 Comparison of ozone profiles

To estimate the quality of CCM results it is also necessary to evaluate not only the total ozone column but also the vertical structure of ozone. In a first step, here we used exemplarily the ozone (ESA) data product derived from the ENVISAT-MIPAS instrument.

The ENVISAT mission with on-board the MIPAS instrument lasted ten years, from the 1st of March 2002 until the 8th of April 2012. Data are available after the commissioning phase from 1st March until July 2002. The Level 2 products consist of a number of geophysical parameters derived from the measured atmospheric limb emission spectra and some instrument auxiliary information. In this case, we used volume mixing ratio (VMR) vertical profile data of ozone derived from MIPAS L2 v7.03 (hereafter called simply L2v7). L2v7 overestimates ozone relative to co-located ozone sonde and lidar measurements, with a magnitude that depends mildly on latitude and pressure. The positive bias is about 5% in the middle and upper stratosphere, and 10-15% in the lower stratosphere.

We checked the mean ozone distribution based on the complete MIPAS-data set from July 2002 and April 2012. In **Figures 7 and 8** the altitude and latitude (zonal mean) dependences is shown, indicating a good agreement between the MIPAS measurements and the EMAC simulation results with respect to the vertical and zonal structure. Some obvious differences are turned out looking at the differences between the ozone data derived from MIPAS and the model results. **Figure 9** (lower parts) indicate that around 100 hPa the MIPAS data may be uncertain due to the detection limit there. In the lower stratosphere the EMAC data are showing slightly higher ozone mixing ratios (about 5-10%). In the middle and upper stratosphere and lower mesosphere MIPAS ozone values are clearly higher than the model data (up to about 20%). For example, the stratospheric ozone maximum in the tropics is underestimated by the model simulations, i.e. about -0.8 ppmv (less than 10%). These first assessments are pointing out that this CCM is absolutely able to reproduce the observed ozone distribution in the middle atmosphere, i.e. above the tropopause up to about 80 km altitude. Longer time series of the vertical structure of ozone are still required to estimate the long-term behaviour of the different height regions, which are, among others, depending on climate change (see also Section 3.4).

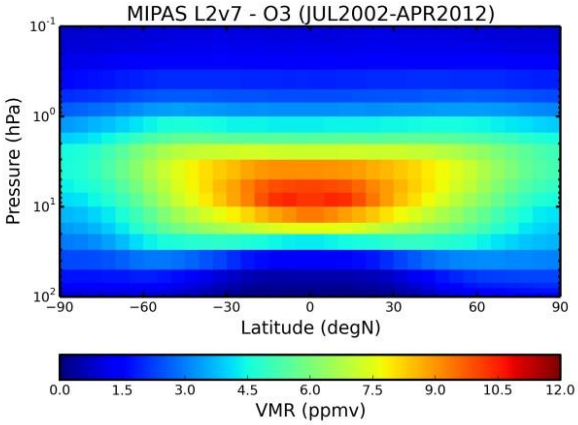

***Figure 7**:* Mean ozone distribution (in volume mixing ratio, VMR) between 100 hPa and 0.1 hPa for the time period between July 2002 and April 2012 derived from the ENVISAT-MIPAS instrument (worked out by Massimo Valeri, guest of DLR, University of Bologna, Italy).

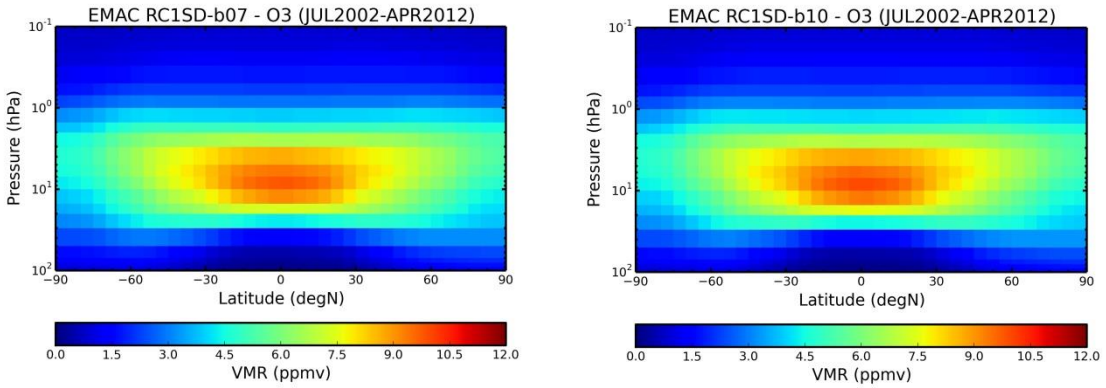

***Figure 8**:* Mean ozone distribution (in mixing ratios) between 100 hPa and 0.1 hPa for the time period between July 2002 and April 2012 derived from the EMAC-RC1SD simulations, left version base-07 (b07), right version base-10 (b10). (Worked out by Massimo Valeri, University of Bologna, Italy.)

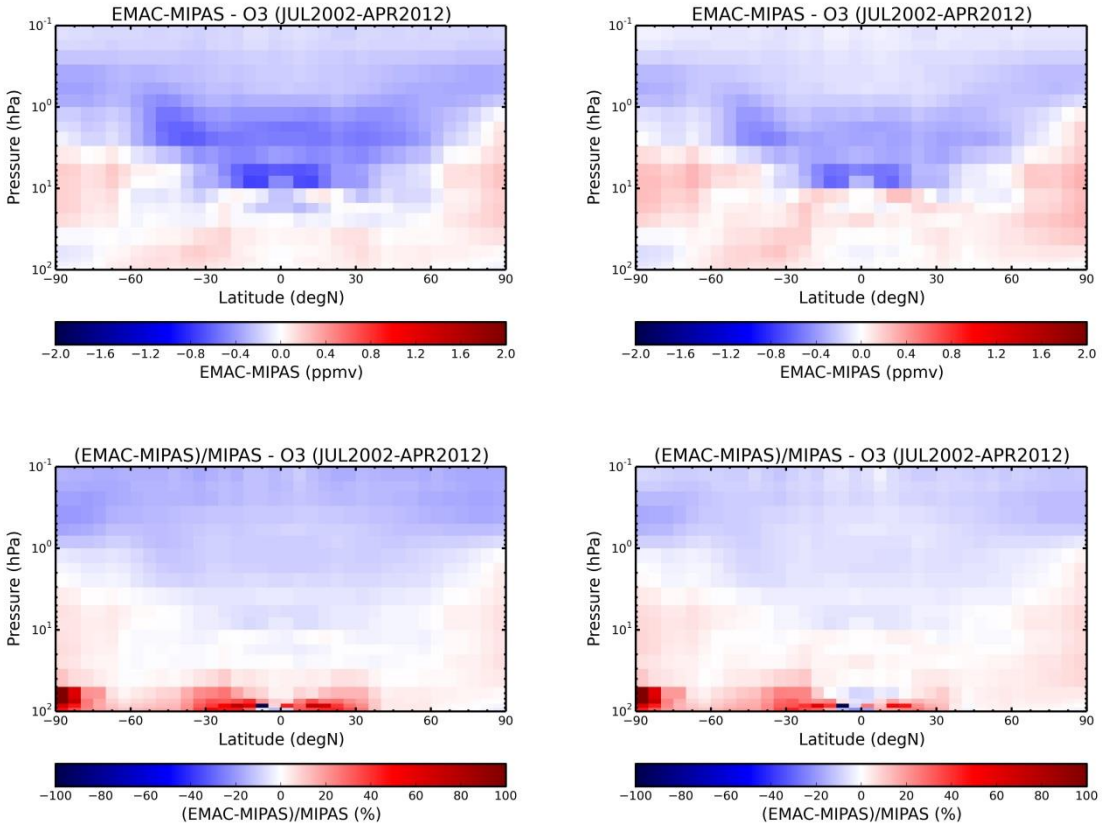

***Figure 9**:* (top) Absolut and (bottom) relative ozone differences between MIPAS and EMAC simulations (left: differences between MIPAS and EMAC RC1SD-b07 and right: differences between MIPAS and EMAC RC1SD-b10).

3.4 Assessment of CCM results and future projections

Figure 10 shows an early example of the temporal evolution of total ozone deviations regarding a mean ozone value (1995-2009) for the near global mean (i.e. global mean values neglecting polar regions). Looking into the past it is obvious that the CCM (here the DLR CCM E39CA, i.e. the predecessor of EMAC) was able to reproduce seasonal and interannual fluctuations in a sufficient manner, although the amplitudes of ozone anomalies are slightly underestimated (Loyola et al., 2009; Dameris and Loyola, 2011). Model data and data derived from satellite observations clearly show the signature of the 11-year solar cycle. The absolute minimum ozone values observed in years 1993-95, which are caused by the eruption of the volcano Pinatubo, are not adequately reproduced by the CCM. The simulated increase in stratospheric ozone amount after year 2010 is a direct consequence of the prescribed decrease of stratospheric chlorine content. The speed at which the ozone layer will rebuild in future depends on a range of other factors, however. Rising atmospheric concentrations of radiatively active gases (such as CO_2, CH_4 and N_2O) do not just cause the conditions in the troposphere to change (i.e. the greenhouse effect warms the troposphere), but also in the stratosphere, which cools down with increasing CO_2 concentrations. The regeneration of the ozone layer thus takes place under atmospheric conditions different to those prevailing during the ozone depletion processes of recent decades. Due to climate change, it is highly unlikely that the ozone layer will return to exactly the way it was before the time of increased concentrations of ozone depleting substances (ODSs). Due to further increasing greenhouse gas concentrations, global atmospheric temperatures will continue to change over the coming decades: It is expected that the troposphere will continue to warm up and that the stratosphere will cool down further due to radiation effects. This will modify chemical processes (i.e. chemical reaction rates) as well as the dynamics (transport and mixing) of the atmosphere (Dhomse et al., 2018; WMO, 2018), which will have different effects in the different stratospheric layers and geographical regions (i.e. low, mid and high latitudes) of the atmosphere (see detailed discussion below).

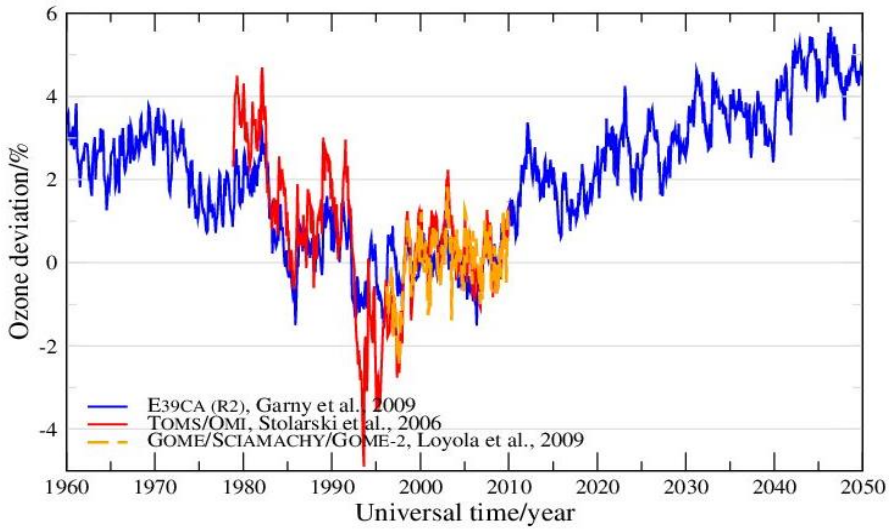

***Figure 10**:* Temporal evolution of the near global mean total ozone column anomaly (60°N to 60°S). The mean annual cycle for 1995 to 2004 is subtracted from satellite measurements (orange and red) and in blue results of the CCM E39CA model simulation R2 (i.e. similar to the REF-C2 simulation discussed before, assuming a moderate climate scenario) from 1960 to 2050 (update of Loyola et al., 2009).

Future prognostics with CCMs also clearly indicate that ozone regeneration will be faster in some areas than in others, where it's quite possible that the recovery of the ozone layer will be delayed (e.g., Dhomse et al., 2018; Keeble et al., 2021; see discussion below). The results of CCM simulations also indicate that the recovery of the ozone layer will vary from region to region and does not represent a simple reversal of the depletion observed over recent years. First examples are presented in **Figure 11**, showing the evolution of the stratospheric ozone layer in the Northern and Southern polar regions (Dameris and Loyola, 2011). In contrast to **Figure 10**, only the data for respective spring months are shown when ozone depletion maximizes. First of all, the CCM E39CA reproduces nicely the different evolution of the ozone layer in the Northern and Southern Hemisphere in the past showing a more pronounced thinning of the ozone layer in the Southern Hemisphere due to the formation of the ozone hole. Interannual fluctuations are well captured by this CCM in the Northern Hemisphere, while they are underestimated in the Southern Hemisphere. Here, for example, the model does not create dynamical situations leading to weak polar vortices in late winter and early spring and therefore higher ozone values as particularly observed in 1988 and 2002. Obviously, the recreation speed of the ozone layer is different in the Northern and in the Southern Hemisphere: In the Northern Hemisphere ozone values found in the 1960ies and 1970ies are reached again around 2030 and further increase afterwards. In the Southern Hemisphere the 2050-values are still below the values found in the 1960ies.

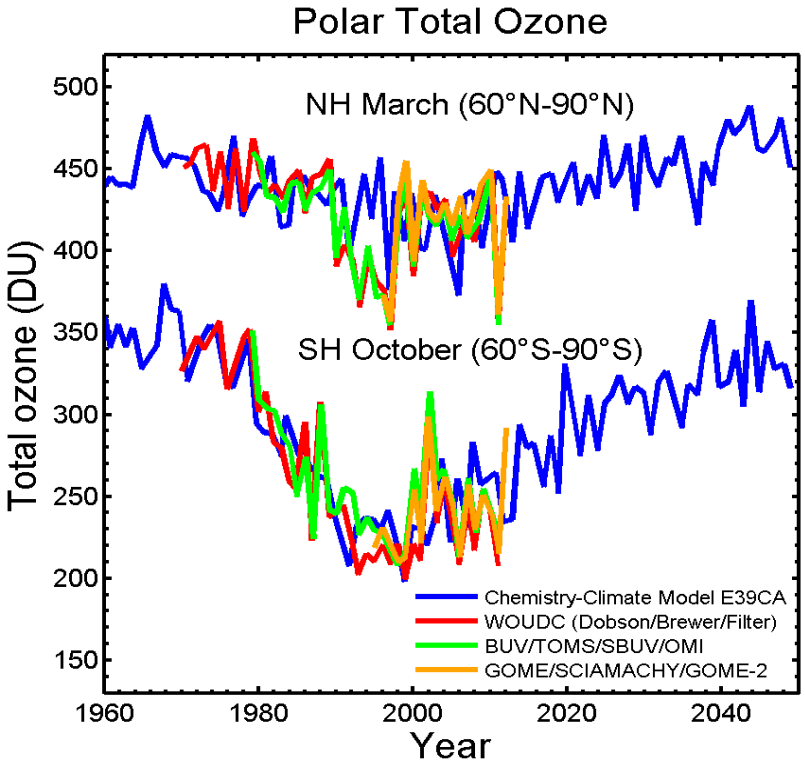

Figure 11: As Figure 10, but now total ozone values for the polar regions (top: Northern Hemisphere for March; bottom: Southern Hemisphere for October). Deviations are given with regard to the mean value of the period 1995-2009 (in %) for the region between 60° and 90°. Notice the different scales on the y-axis.

In the last years, the SPARC/IGAC Chemistry-Climate Model Initiative (CCMI) has been established as successor of the SPARC CCMVal activity. Among others it has been initiated to support the last “WMO Scientific Assessment of Ozone Depletion”, which was published in late 2018 (WMO, 2018). New model simulations with updated (further developed) CCMs were proposed. For instance, three different sets of reference simulations were suggested by CCMI, namely free-running hindcast simulations from 1960 to 2010 (REF-C1), hindcast simulations with specified dynamics (SD) from 1980 to 2010 (REF-C1SD), and combined free-running hindcast and projection simulations from 1960 to 2100 (REF-C2, assuming a moderate enhancement of greenhouse gas concentrations, i.e. RCP6.0). The hindcast simulations with specified dynamics were branched off from restart files (1 January 1979) of the corresponding free-running hindcast simulations and “nudged” by Newtonian relaxation towards ERA-Interim reanalysis data, which are available with a 6-hourly time resolution from the year 1979 onwards. In this connection the CCM EMAC carried out these reference simulations (some results of the RC1SD simulations have been presented already in Sections 3.2 and 3.3). A comparison of these model data derived from the reference simulations were used to confront them with updated ESA Ozone_cci GOME-type Total Ozone Essential Climate Variable, which were completed with OMI data (GTO-ECV_OMI). In the following some of the results are presented, which also were submitted for the common model exercise

prepared for the ozone assessment report (Dhomse et al., 2018). They mostly confirmed our recent findings, which were published some years ago. An improved future assessment of the ozone layer with EMAC until 2100 (REF-C2) was presented, allowing to distinguish in detail between different geographical regions.

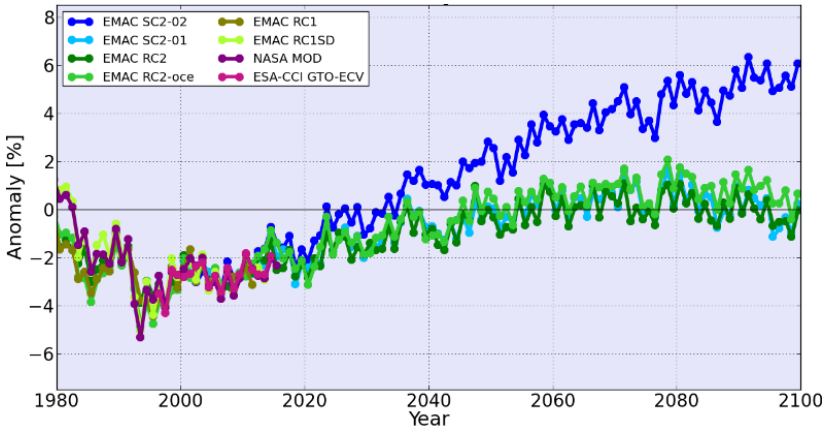

***Figure 12**:* Temporal evolution of the near global mean total ozone column anomaly (60°N-60°S). Anomaly values are related to the mean from 1960 to 1980. In addition to the three EMAC reference simulations (RC2=REF-C2, in dark green; RC2-oce=REF-C2 coupled with a mixed layer ocean, in medium green; SC2-01=REF-C2 with a reduced vertical resolution, in light blue; all three simulations are under RCP6.0 conditions), the dark blue line (SC2-02) is showing in comparison the results of a sensitivity simulation under RCP8.5 conditions. Further, the ESA-CCI data products (in pink) and the data product prepared by NASA (1979 to 2015, in purple) are compared with respective model simulations (RC1=REF-C1, in olive-green and REF-C1SD=RC1SD, in light green) representing the past.

Figure 12 illustrates the good agreement between the model results and the NASA and ESA data set derived from observations. This is the foundation for a robust prediction of the recovery of the ozone layer. Based on this model assessment it is obvious that a full recovery of the near-global mean total ozone column can be expected around 2035. This date is earlier than expected with respect to the decline of the stratospheric chlorine content due to the regulations of ozone depleting substances in the Montreal protocol. The major reason for this behaviour is the impact of climate change (stratospheric cooling and modifications of the circulation). The possibility of a “super-recovery” of the ozone layer after about 2045 is also the results of stratospheric changes caused by enhanced greenhouse gas concentrations.

Figure 13 shows the different behaviour in Arctic and Antarctic region. Here the results are given for the spring season (March and September, respectively) indicating strongest ozone depletion particularly in the 1990 and 2000s. The largest negative anomaly is identified in the South Polar Region, i.e. the ozone hole phenomenon. Back to normal ozone content is predicted after about 2030 (with respect to the RCP6.0 climate scenario) in the North Polar Region, whereas the

ozone hole will be closed around 2060. It turned out that the Antarctic lower stratosphere is not obviously affected by climate change with respect to the ozone depleting chemical reactions. A further cooling of this stratospheric region is of no significant importance for the amount of ozone destruction because it is already very cold there and therefore a complete activation of ozone depleting substances is already observed now.

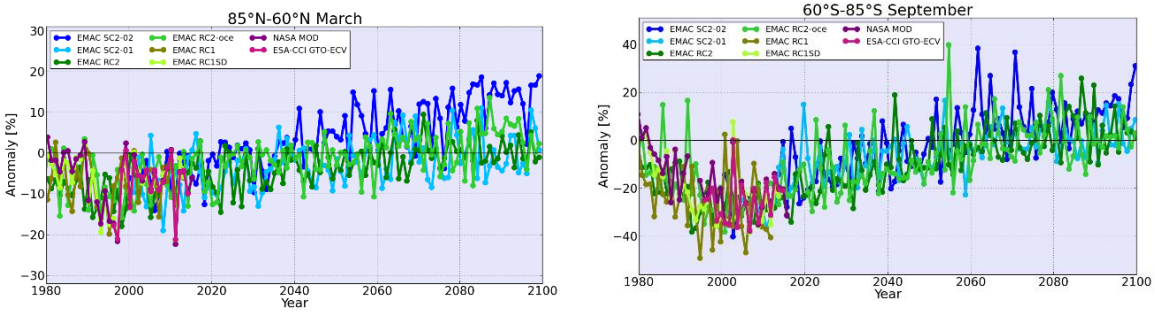

Figure 13: Temporal evolution of the total ozone column anomalies in the North (left) and South polar region (right) during the spring months March and September. Anomaly values are related to the mean from 1960 to 1980. For descriptions of the different color lines please have a look on the caption of Figure 12.

Based on the observations over the Antarctic region in September, a first sign of a beginning ozone recovery is detected (Solomon et al., 2016; more discussion about the statistical significance of the respective analyses can be found in WMO, 2018). The EMAC results show a consistent reaction.

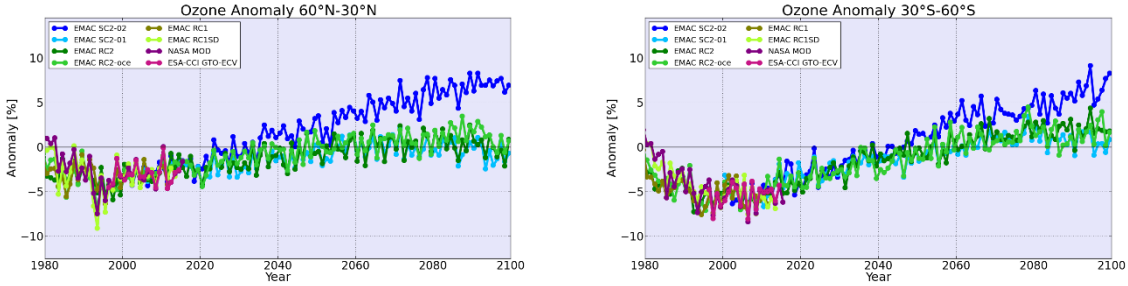

Figure 14: Similar to Figure 12, but now for the mid-latitude regions in the Northern (left) and Southern hemisphere (right).

At Northern mid-latitudes the EMAC REF-C2 simulation indicates a full recovery in these days, but one has to consider the large interannual variability in this region. The model results for the mid-latitudinal region in the Southern hemisphere show a return to undisturbed total ozone values around 2035. Both geographical regions imply a super-recovery of the ozone column in the second half of this century.

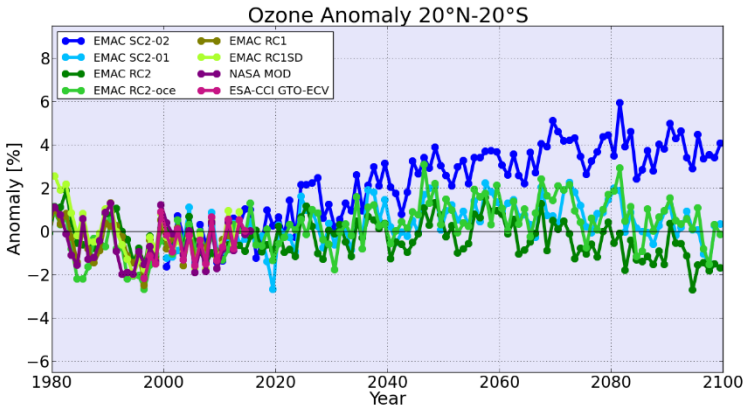

Figure 15: Similar to Figure 12, but now for the tropical region.

As pointed out in Section 3.1 (see Figure 3) there may be the possibility for a future reduction of the tropical total ozone column with implication for the UV-B content near the surface. The EMAC REF-C2 simulation indicates the same future behaviour (**Figure 15**). In the following, results of a former investigation of the possible future evolution of the tropical ozone layer was presented by Meul et al. (2016).

3.5 A first investigation of tropical ozone in future

In particular, future projections of tropical total column ozone (TCO) are challenging, as its evolution is affected not only by the expected decline of ozone depleting substances but also by the uncertain increase of greenhouse gas (GHG) emissions. To assess the range of tropical TCO projections, CCM simulations forced by three different GHG scenarios (Representative Concentration Pathway (RCP) 4.5, RCP6.0, and RCP8.5) were analysed. It was found that tropical TCO will be lower by the end of the 21st century compared to the 1960ies in all scenarios with the lowest TCO value in the medium RCP6.0 scenario in the 2090ies (**Figure 16**). Uncertainties of the projected TCO changes arise from the magnitude of stratospheric column decrease and tropospheric ozone increase, which both strongly vary between the scenarios. In the three scenario simulations the stratospheric column decrease is not compensated by the increase in tropospheric ozone. The concomitant increase in harmful ultraviolet irradiance reaches up to 15% in specific regions in the RCP6.0 scenario. For more details see Meul et al. (2016). The results of this study were supported by similar analyses presented in Dhomse et al. (2018); see also the discussions in WMO (2018).

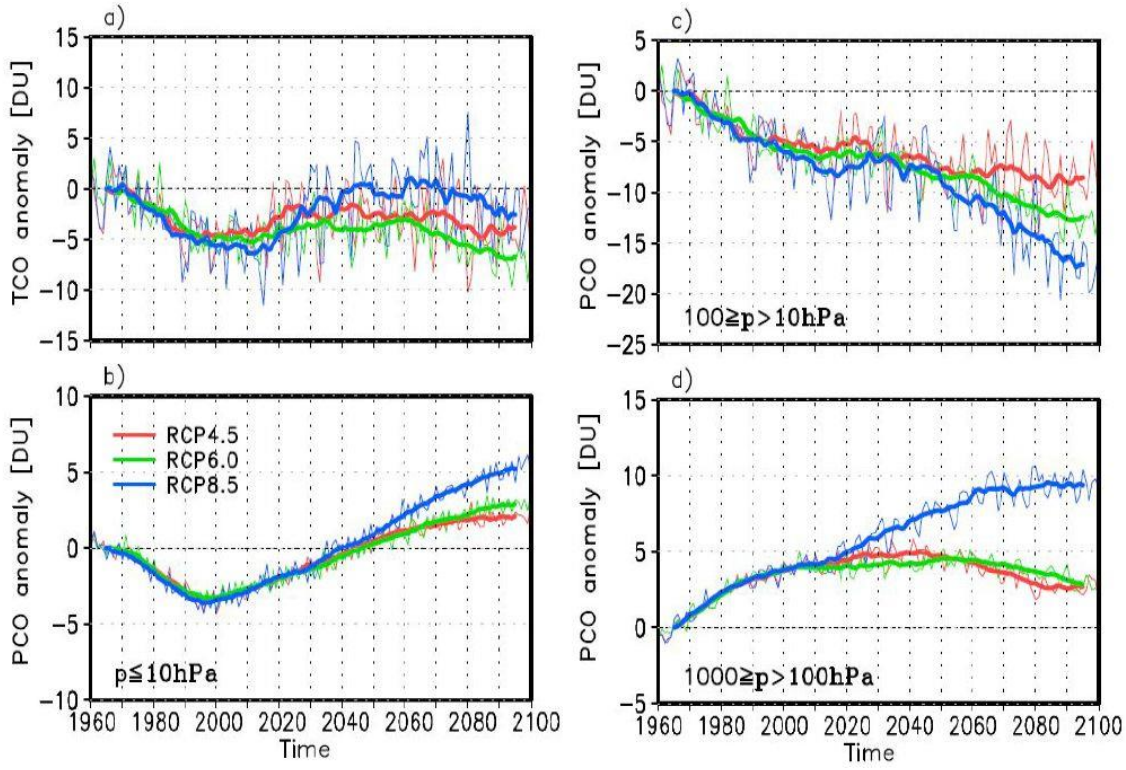

Figure 16: (a) Time series of annual mean tropical mean (20°S-20°N) total ozone column (TCO) anomaly to the 1960-1970 mean for the RCP4.5 (red), RCP6.0 (green), and RCP8.5 (blue) simulations, (b–d) same as (a) but for the partial ozone column (PCO) for the (b) upper stratosphere (pressure ≤ 10 hPa), (c) middle stratosphere (100 hPa ≥ pressure > 10 hPa), and (d) troposphere (1000 hPa ≥ pressure > 100 hPa). Thick solid lines indicate the smoothed time series (figure taken from Meul et al., 2016).

3.6 A health check of the ozone layer at global and regional scales

The first version of the ESA Ozone_cci Gome-type Total Ozone Essential Climate Variable (GTO-ECV) data record (Coldewey-Egbers et al., 2015) was used to calculate spatially resolved ozone trend and variability patterns based on the 18-year period from June 1995 to June 2013 (Coldewey-Egbers et al., 2014). This comprehensive global long-term data set enables us to disentangle the various sources of ozone variability and its drivers by multivariate linear regression. The regression model quantifies the relationship between ozone and several explanatory variables describing natural and/or anthropogenic forcing. We adopted the form according to Vyushin et al. (2007) and included – in addition to the seasonal cycle and a linear trend term - the quasi-biennial oscillation (QBO) signal (represented by both 30 hPa and 50 hPa equatorial zonally averaged winds), the 10.7cm radio flux accounting for the solar cycle impact, and the Multivariate El Niño-Southern Oscillation Index (MEI).

The annual mean linear trend coefficients are calculated for the region 60°N to 60°S and are shown in **Figure 17**, left panel. Grey crosses denote regions where the

trends are not statistically significant. Estimated trends are positive (yellow and red shading) in major parts of the globe. Small areas indicating nonsignificant negative trends are found in the northern middle latitudes and in the southern Indian Ocean around 30°E-90°E. Largest positive trends of about 1.5-2% per decade are found in the Northern Hemisphere in the European and North Atlantic region, but they are statistically significant in limited small areas only. In southern middle latitudes significant trends of about 1.5% per decade are found around southern South America, Australia, and New Zealand. Thus, the expected onset of ozone recovery in the middle latitudes is still only on the edge of detection.

However, the GTO-ECV data record shows significant positive trends around 1% per decade in large parts of the tropics and subtropics. In order to explain the physical mechanisms that control interannual variability and thus small trends in the tropics, we discuss now the link between the El Niño-Southern Oscillation (ENSO) phenomenon and total ozone as well as lower stratospheric temperature and tropopause pressure.

The correlation between MEI and total ozone is negative for almost the entire tropical zone except the eastern Indian Ocean and Southeast Asia, which means that ozone values are higher than the mean during La Niña cold phases and lower during El Niño warm phases. Five to 15 DU of ozone variability can be explained by this phenomenon in those regions. The longitudinal structure in the tropics can be explained with a shift in the convection pattern from east to west during warm El Niño events. The same correlation pattern is found for the lower stratospheric temperature at 100 hPa. Negative correlation between MEI and temperature means that temperature is increasing during ENSO cold events (when temperature in the lower tropical troposphere is decreasing), and temperature is decreasing during ENSO warm events (when temperature in the lower tropical troposphere is increasing). This anticorrelation between troposphere and stratosphere is related with respect to enhanced tropical upwelling and a strengthened Brewer-Dobson circulation during El Niño events (Calvo et al., 2010). Furthermore, we calculated the linear trend term for tropopause pressure (pressure at 395 K potential temperatures). The trend pattern shows some agreement with the ozone trend over the Pacific, southern South America, and the North Atlantic region. Positive pressure trends indicate that a descending tropopause is associated with an expanding stratosphere and hence increasing ozone levels. In the tropics tropopause pressure decreases (ascending tropopause) during ENSO warm events - leading to reduced stratospheric ozone amounts - and tropopause pressure increases (descending tropopause) during ENSO cold events leading to enhanced stratospheric ozone amounts.

With regard to the detected ENSO-related correlations the observed regional trends in the tropics for ozone, temperature, and pressure can now be explained having a look at the MEI time series itself for the period 1995 to 2013. We conclude that a strong ENSO warm event 1997/1998 at the beginning of the fit period and a strong ENSO cold event 2010/2011 at the end of the fit period, and hence the apparent

negative trend in ENSO toward cold events, induce the derived changes in the atmospheric parameters in this region.

The right panel of **Figure 17** shows the year, in which we can expect to detect a total ozone trend of a given magnitude (according to Weatherhead et al., 1998, their Equation (3)). We use the variance and autocorrelation determined from the GTO-ECV record, and we use model projections for the first half of this century to obtain a zonal distribution of expected ozone trends, which are smallest in the tropics (~0.5% per decade) and increase toward higher latitudes. Values in middle latitudes of the Southern Hemisphere (1–2% per decade) are expected to be slightly larger than in the Northern Hemisphere (0.7–1.7% per decade). The plot indicates that detection of changes in the tropics will not be possible before 2030, because the expected trend itself is small and autocorrelation is not negligible. On the other hand, variability is low in this region. Toward higher latitudes the number of years decreases. Early trend detection will be possible from ~2015 onward in some regions in the Southern Hemisphere (20°S poleward), whereas in the Northern Hemisphere stronger interannual and intra-annual variabilities lead to longer periods needed to observe a recovery of ozone (trend detection possible from 2020 onward).

As can be readily seen from the results the length of the current GTO-ECV data records covering 18 years is still at the lower end for reliable recovery detection as natural variability still dominates the evolution of total ozone in middle latitudes since the mid-1990s. Therefore, trend estimates presented in **Figure 17** (right) are not significant in major parts of the extra-tropics.

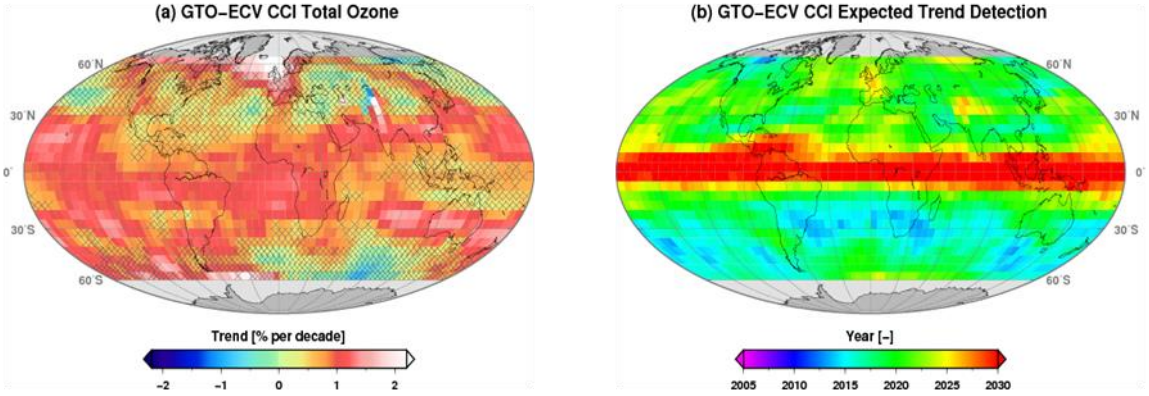

***Figure 17*:** Left: total ozone trend [%/decade] and right: year of expected trend detection.

Thus, our results clearly indicate a need for continuous monitoring of ozone and an extension of the current data records using future missions in order to (1) detect the expected success of the Montreal Protocol and (2) achieve a better understanding of the interaction and feedback mechanisms between ozone and climate change.

We are currently working on an update of this exercise, which also includes the regional trends will include, but then currently from 1995 to 2022. There will also be an analysis of the give seasonal variability of trends.

3.7 The QBO signal in model data and observations

Attributing variability is a key element of a reliable trend analysis. One example of a dominant mode of variability is the quasi-biennial oscillation (QBO) in tropical zonal mean zonal wind. Recurring westerly and easterly phases of the dominant zonal wind directions are associated with characteristic horizontal and vertical ozone distributions. A spectral band-pass filter is a convenient way to extract the QBO associated changes in ozone and to compare the patterns between model implementations and observational data. A QBO signal exists in column data and in profile data of ozone. The complementary use of column and profile data will be discussed.

Starting with column data we use results derived from the CCM EMAC simulations (Jöckel et al., 2016). A number of model integrations simulated the climate and composition of the recent past using free running and *nudged* configurations of EMAC (see Section 3.4). **Figure 18** shows band-pass filtered ozone and ozone variability on longer time scales in each panel. The panel on the upper left of **Figure 18** shows results for ERA-Interim column ozone. Note that for the nudging of the EMAC model (lower left panel in **Figure 18**) ERA-Interim meteorological data has been used. Thus the expectation should be, that if the assimilation for ozone works well in ERA-Interim and the ozone in the REF-C1SD integration is well represented we should find good agreement (which we do). In the free running model (REF-C1) the circulation constraint is weaker and thus the amplitude of ozone anomalies seems to be smaller (lower right panel in **Figure 18**). However, the purely observational data set (upper right panel in **Figure 18**) is showing a similar behaviour (note the optical caveat that the observational data has a smaller latitudinal extent).

Figure 19 shows latitude-pressure cross-sections of ozone volume mixing ratio composites (see definition in the figure caption). There is a clear vertical structure in the tropical ozone caused by the QBO (as indicated by the two maxima/minima at the equator) and the QBO related ozone changes extend far beyond the narrow latitudinal range that is dominated by the zonal mean zonal wind reversal. Considering the sampling issues of the satellite product there is good agreement between the REF-C1SD simulation and the SCIAMACHY observations.

A side product of the band-pass filtered data is a delineation of variability on longer time scales, including the ENSO signal. The study by Kunze et al. (2016) discussed the interplay of the Monsoon and ENSO modulations on UTLS composition. The Monsoon (here: the Indian summer monsoon) is an important modulator of composition on the annual time scale, however it shows also interannual variability and some co-variability with the ENSO (see also Coldewey-Egbers et al. (2014) for details on ENSO ozone variability). Further studies are required to disentangle the variability on longer time scales and to interpret the spectrum of “slow” variability better (as illustrated in **Figure 18** in the lower part of the individual panels).

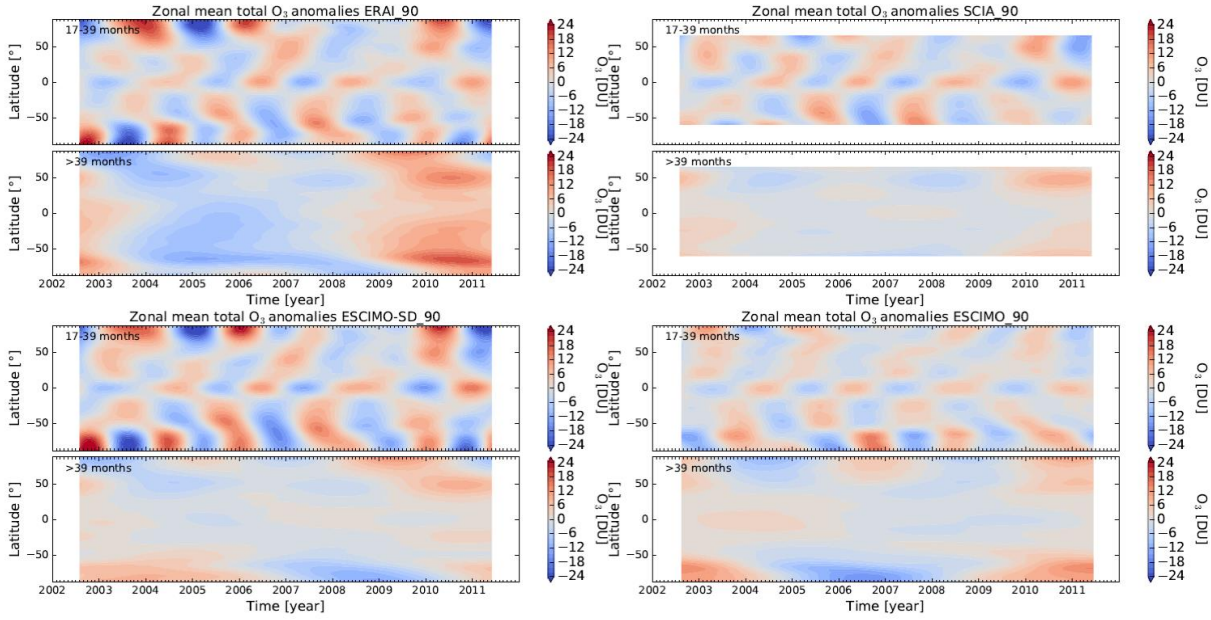

Figure 18: Filtered column ozone data for ERA-Interim (upper left), the SCIAMACHY ozone CCI data set (upper right), REF-C1SD simulation (lower left), and REF-C1 free running simulation (lower right). In each category there a two panels. The upper panel shows the QBO related variability the lower panel the longer time scales. (The residuals on short time scales are not shown.)

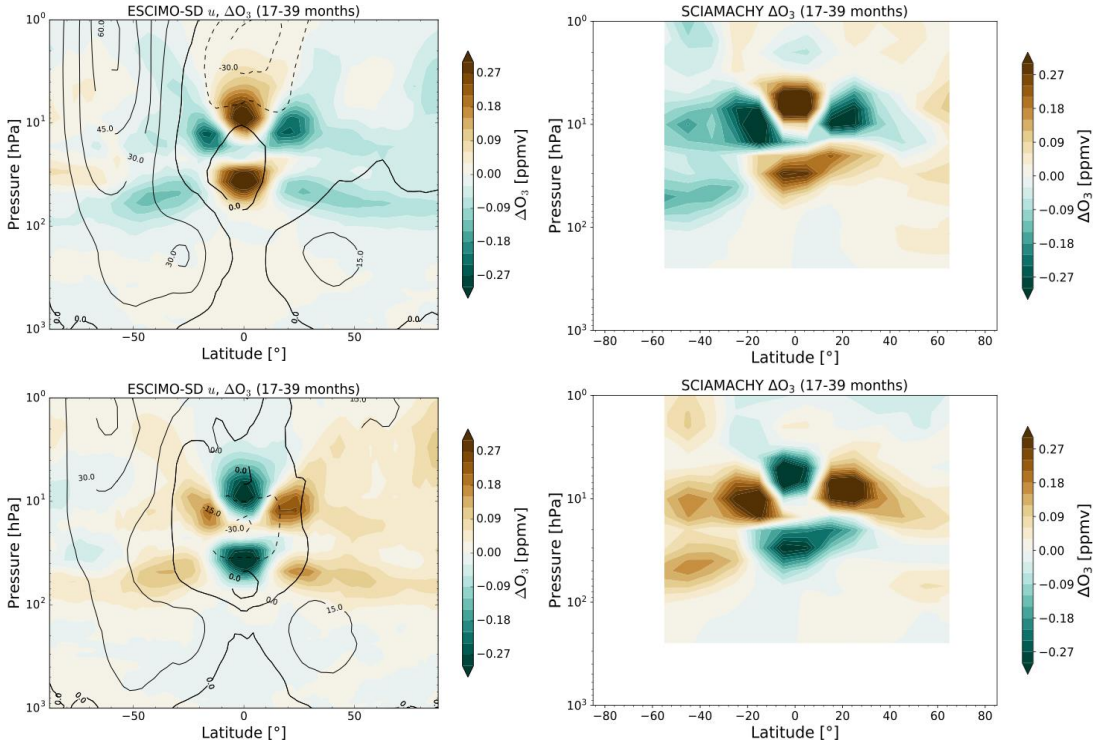

Figure 19: Latitude-pressure cross-sections of ozone volume mixing ratio composite differences for the times when the filtered column ozone data (Figure 16) has a maximum (top row) and when it has a minimum (bottom row) for the REF-C1SD simulation (left column) and the satellite observations from SCIAMACHY (right column).

A more detailed investigation about teleconnections of the QBO in a multi-model ensemble of QBO-resolving models (incl. EMAC) was published in the meantime by Anstey et al. (2021). Beside the results of 11 models, they used different datasets of reanalyses covering the indicated periods: ERA-Interim (1979–2018), ERA-40 (September 1957 to August 2002), ERA-20C (1900–2010), MERRA-2 (1980–2018), and JRA-55 (1958–2018).

3.8 Ozone variability in EC Earth-TM5 coupled climate simulations

The Earth System Model EC Earth (Hazeleger et al., 2012) has been further developed for the recent round of model simulations in support of the IPCC assessment report (AR6 / CMIP6**;** Döscher et al., 2021). The historical forcing data and scenarios are provided to the climate modelling community, and were implemented in EC Earth.

Model simulations including coupling with ozone are available through EC-EARTH seasonal simulations. Focus for the CRG study with EC Earth in Ozone_cci was a study on the importance of interactive vs. prescribed ozone. The ozone profile spatial and temporal variability of these simulations in the UT/LS were confronted to the variability in the Ozone_cci climate data records.

The new EC Earth model version (EC Earth V3.2; IFS cy36r4 TL255, linearly reduced Gaussian grid equivalent to 512 x 256 longitude/latitude; 91 levels; top level 0.01 hPa; NEMO3.6, ORCA1 tripolar primarily 1 degree with meridional refinement down to 1/3 degree in the tropics; 362 x 292 longitude/latitude; 75 levels; top grid cell 0-1 m), sea Ice: LIM3) contains many model improvements compared to V2. One key extension crucial for ozone-climate interactions is the model top upward extension to include the stratosphere and mesosphere up to 0.01 hPa. Also important is the amount of vertical layers, which has been increased from 62 to 91 levels. The new sub-km vertical resolution in the UT/LS is considered a major improvement for process studies on ozone profile - climate interactions.

EC Earth is coupled to the TM5 chemistry-transport model, which is currently ran at 3x2 degrees spatial resolution and 34 layers. Two-way coupling of ozone between EC Earth and TM5 has been implemented, i.e. the ozone, which is being transported and is chemically reacting and deposited in TM5, is used in IFS in the radiation schemes, while the meteorological wind and temperature fields from IFS are used to drive the transport in TM5. Updates of the coupled model system were published (Noije et al., 2014; 2020).

The CMIP6 prescribed 3-D ozone distribution for the period 1850-2014 that has been released in 2016 for use in preparation of the climate simulations for the next IPCC report. The CMIP6 ozone was implemented both in IFS for non-coupled climate runs with EC Earth and in TM5 for the coupled chemistry-climate simulations. The CMIP6 ozone profile distribution has been compared with the cci-based total column ozone observations (MSR-2 multi-decadal record) and shows overall consistency.

As an example, **Figure 20** shows a latitude-height comparison between the CMIP6 zonal-mean distribution for 2010 (DJF) and the MSR-2 observations for the same months and distributed vertically to the standard Fortuin and Kelder (1998) climatological vertical profile as used in TM5. More comparisons between CMIP6 ozone and other Ozone_cci climate records are still to be made.

The key difference between the non-coupled EC Earth simulations using IFS only and the simulations with IFS coupled to TM5 is the dynamic ozone transport in the tropopause region in TM5. While the 3-D ozone distribution is prescribed in IFS and its radiation routines the simulations coupled with TM5 will use the 3-D ozone distribution from TM5 in the radiation routines and thus ozone changes may affect the UT/LS circulation. In TM5 ozone is not prescribed though nudged to the CMIP6 ozone fields and only (well) above the tropopause. In the tropics (30°S-30°N) stratospheric ozone is nudged for pressures < 45 hPa, whereas in the extra-tropics ozone is nudged for pressures < 90 hPa to account for differences in the height of the tropopause. The relaxation times applied are 2.5 and 4 days for the tropics and extra-tropics, respectively. Consequently, the magnitude of stratosphere-troposphere exchange (STE) in TM5 depends on the strength of the overturning circulation determined by the climate model which will depend on the climate forcing and

subsequent climate change. The change in STE will affect the tropospheric ozone budget and chemistry of the upper troposphere. Because stratospheric chemistry is lacking in TM5 there is not a full coupling of the general circulation to mid-upper stratospheric ozone changes in these simulations and thus with EC-Earth/TM5 focus is given on UT/LS ozone-climate couplings.

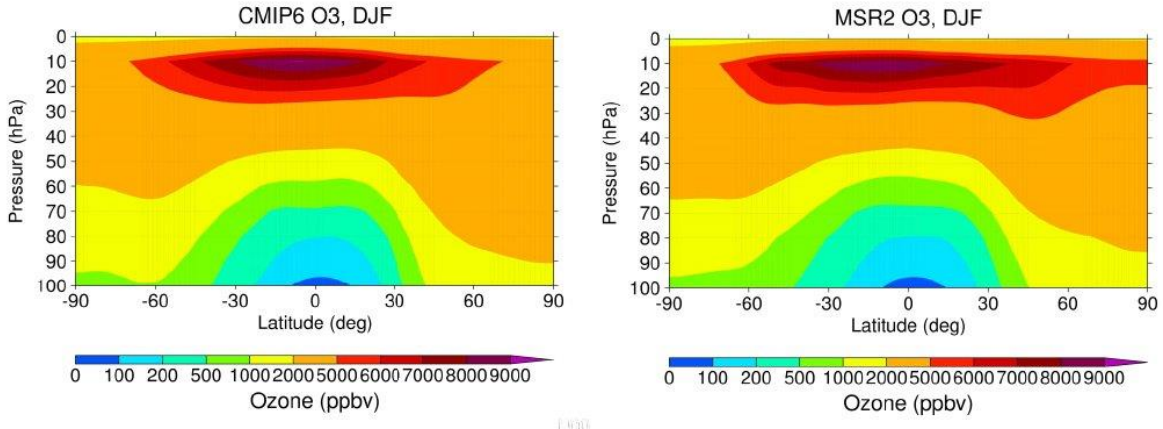

Figure 20: Comparison of latitude-height cross section analysis for ozone volume mixing ratio between the CMIP6 zonal-mean distribution for 2010 (DJF) and the MSR-2 observations for the same northern winter months.

One key question for ozone-climate interactions is the importance of ozone short-term variability in the UT/LS. There are some indications in the scientific literature that suggest a potential large impact of ozone variability, e.g. through studying the impact of zonal asymmetries in ozone (McCormack et al., 2011; Albers et al., 2012). By comparison of seasonal northern hemisphere winter simulations with interactive ozone to simulations with prescribed (zonal-mean) CMIP5/CMIP6 forcing the importance of ozone variability for climate and atmospheric circulation in the new version of EC Earth were diagnosed. The realism of the ozone profile variability in the interactive simulations were evaluated using the Phase-2 Ozone_cci ozone profile extended climate data records.

Further efforts have been made in the last years, concerning the comparison of tropospheric ozone reanalysis products (e.g., Huijnen et al., 2020). Global tropospheric ozone reanalyses on the basis of different state-of-the-art satellite data assimilation systems have been created, as part of the Copernicus Atmosphere Monitoring Service (CAMS) as well as two independent reanalyses (Tropospheric Chemistry Reanalysis, i.e. TCR-1 and TCR-2). They were compared and evaluated for the past decade. The CAMS reanalysis is the global reanalysis dataset of atmospheric composition produced by the European Centre for Medium-Range Weather Forecasts (ECMWF), consisting of three-dimensional time-consistent atmospheric composition fields, including aerosols and chemical species (Inness et al., 2019). The chemical mechanism of the ECMWF's Integrated Forecast System (IFS) is a modified and extended version of the Carbon Bond 2005 chemistry scheme

(CB05; Yarwood et al., 2005), a chemical mechanism for the troposphere, as implemented in the chemistry-transport model TM5 (Huijnen et al., 2010). CB05 describes tropospheric chemistry with 55 species and 126 reactions. Stratospheric ozone chemistry in IFS(CB05) is parameterized by a so-called “Cariolle-scheme”. For instance, **Figure 21** demonstrate that the updated chemical reanalyses agree well with each other for most cases, which clearly show the usefulness of the these chemical reanalyses in a variety of studies. The elaborations of Huijnen et al. (2020) indicated that improving the observational constraints, including the continued development of satellite observing systems, together with the optimization of model parameterizations such as deposition and chemical reactions, will lead to increasingly consistent long-term reanalyses in the future.

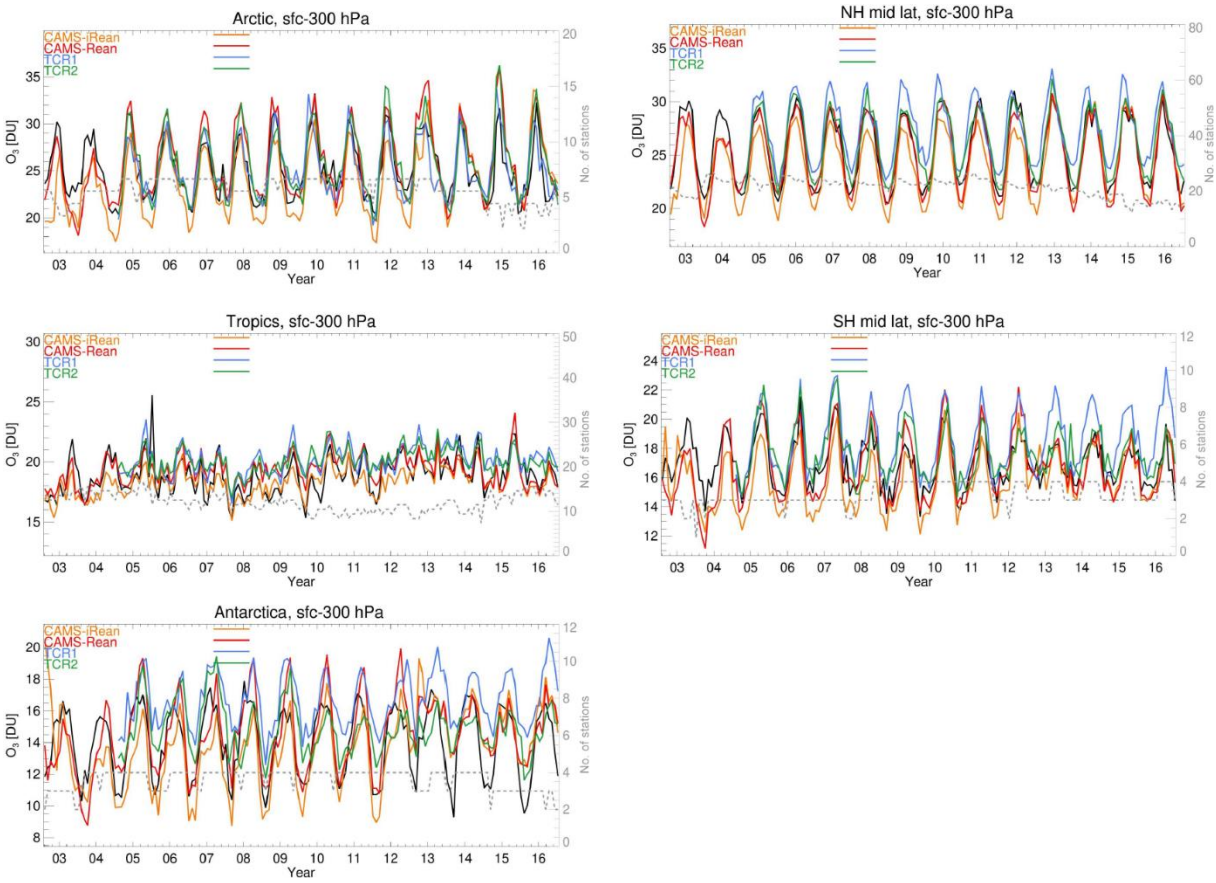

Figure 21: Evaluation of zonally averaged monthly-mean partial columns (surface to 300 hPa) against sonde observations. Observations are in black. The dashed grey line refers to the number of stations that contributes to the statistics (right vertical axis). (The figure is taken from Huijnen et al., 2020).

3.9 Extension of GTO-ECV forward and backward in time

As part of the first phase of the ESA-CCI+ ozone project the GTO-ECV data record has been expanded (i) forward as well as (ii) backward in time. Both versions will enable us to further extend and improve investigations related to the long-term evolution of ozone.

(i) In addition to the existing pool of satellite sensors included in GTO-ECV (GOME/ERS-2, SCIAMACHY/ENVISAT, OMI/Aura, GOME-2/MetOp-A, and GOME-2/MetOp-B) measurements from the Tropospheric Monitoring Instrument (TROPOMI), launched in October 2017 on board the Sentinel-5 Precursor (S5-P) satellite platform, have been included. TROPOMI level-2 data were first converted into a daily level-3 product and then carefully adjusted with respect to the GTO-ECV reference sensor OMI/Aura as a function of latitude and time. The updated GTO-ECV data record now covers the 25½ year period from July 1995 through December 2020. **Figure 22** shows total ozone columns as a function of latitude and time from 1995 to 2020.

(ii) Regarding the extension backward in time, we use the adjusted MERRA-2 (Modern Era Retrospective Analysis for Research and Applications version 2) reanalysis total ozone data set, produced at the National Aeronautics and Space Administration (NASA) Global Modeling and Assimilation Office (GMAO), that covers the period 1980 to 2018 (Bosilovich et al., 2015). Compared to the MERRA-2 data set, the adjusted version used here has been corrected by "normalizing" back to the complete SBUV record (1979 onwards) using the long-term ozone record found in the Merged Ozone Data Set (MOD; Frith et al., 2014, 2017) in order to improve its long-term coherence.

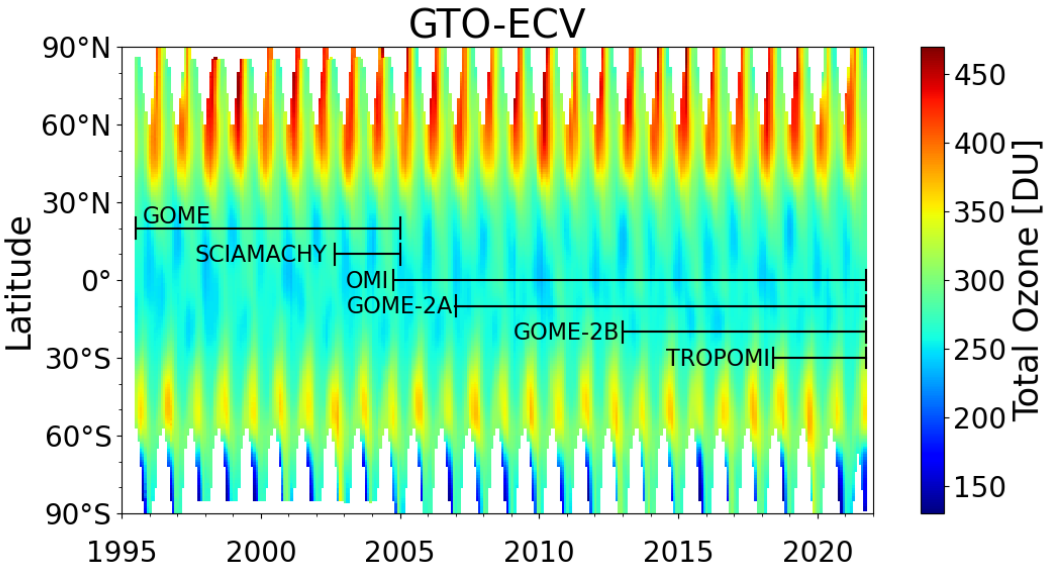

***Figure 22*:** GTO-ECV total ozone column as function of latitude and time from 1995 to 2020.

As a baseline for the combination of GTO-ECV and the adjusted MERRA-2 we use the results from an extensive comparison of both records (Coldewey-Egbers et al., 2020). Total ozone columns and associated standard deviations show a very good agreement in terms of both spatial and temporal patterns during their 23-year overlap period from July 1995 to December 2018. The mean difference between adjusted MERRA-2 and GTO-ECV 5° × 5° monthly mean total ozone columns is −0.9±1.5%.

A small overall negative drift in the differences for almost all latitude bands does not exceed 1% per decade. Ozone anomalies and the distribution of their statistical moments indicate a very high correlation among both data records as to the temporal and spatial structures. Furthermore, the consistency of the data sets was evaluated by means of an empirical orthogonal function (EOF) analysis. The interannual variability is assessed in the tropics, and both GTO-ECV and adjusted MERRA-2 exhibit a remarkable agreement with respect to the derived patterns. The first four EOFs can be attributed to different modes of interannual climate variability, and correlations with the Quasi-Biennial Oscillation (QBO), the El Niño–Southern Oscillation (ENSO) signal, and the solar cycle were found.

Before combining GTO-ECV and the adjusted MERRA-2, the latter is further corrected as a function of latitude and time in order to match GTO-ECV columns and to remove possible biases and seasonal dependences. **Figure 23** shows total ozone columns of the harmonized GTO-ECV and adjusted MERRA-2 record as a function of latitude and time from 1980 to 2020.

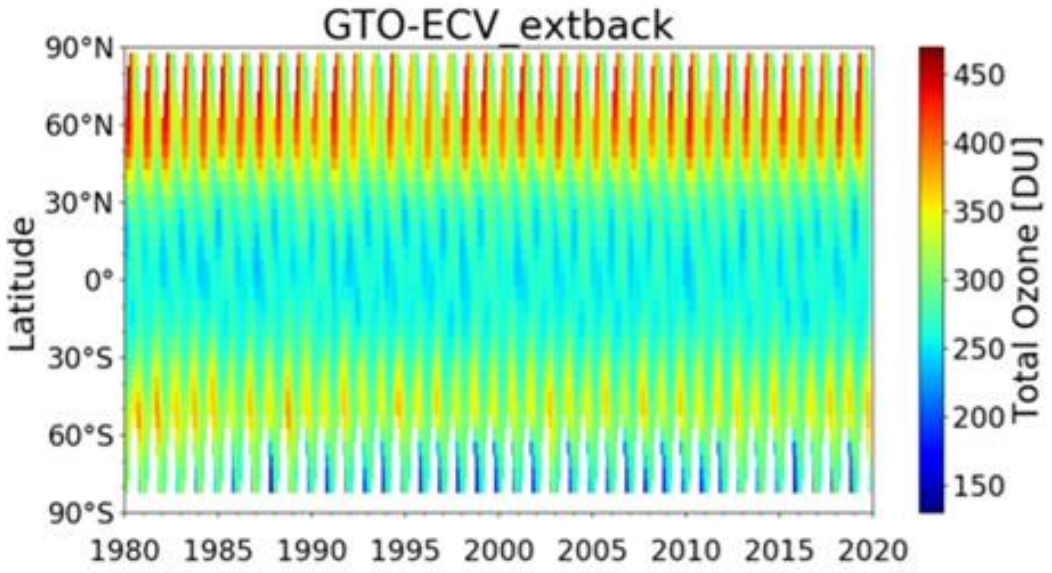

Figure 23: GTO-ECV extended backward in time using adjusted MERRA-2 reanalysis data; total ozone column as a function of latitude and time from 1980 to 2020.

It is worth noting that the GTO-ECV data was used in the current IPCC-report 2021 (see https://www.dlr.de/eoc/en/desktopdefault.aspx/tabid-17417/27631_read-74125/).

3.10 The extraordinary situation in northern spring 2020

Ozone data from July 2019 to April 2020 from the Tropospheric Monitoring Instrument (TROPOMI) sensor on board the EU/ESA Copernicus Sentinel-5 Precursor satellite are scientifically used for the first time in combination with the long-term ozone data set from the European satellite data record GOME-type Total

Ozone Essential Climate Variable (GTO-ECV) from July 1995 to June 2019 (Coldewey-Egbers et al., 2015).

Ozone data derived from the TROPOMI sensor on board the Sentinel-5 Precursor satellite show exceptionally low total ozone columns in the polar region of the Northern Hemisphere (Arctic) in spring 2020. Minimum total ozone column values around or below 220 Dobson units (DU) were seen over the Arctic for 5 weeks in March and early April 2020 (**Figure 24**). Usually the persistence of such low total ozone column values in spring is only observed in the polar Southern Hemisphere (Antarctic) and not over the Arctic. These record low total ozone columns were caused by a particularly strong polar vortex in the stratosphere with a persistent cold stratosphere at higher latitudes, a prerequisite for ozone depletion through heterogeneous chemistry. Based on the ERA5, which is the fifth generation of the European Centre for Medium-Range Weather Forecasts (ECMWF) atmospheric reanalysis, the Northern Hemisphere winter 2019/2020 (from December to March) showed minimum polar cap temperatures consistently below 195 K around 20 km altitude, which enabled enhanced formation of polar stratospheric clouds.

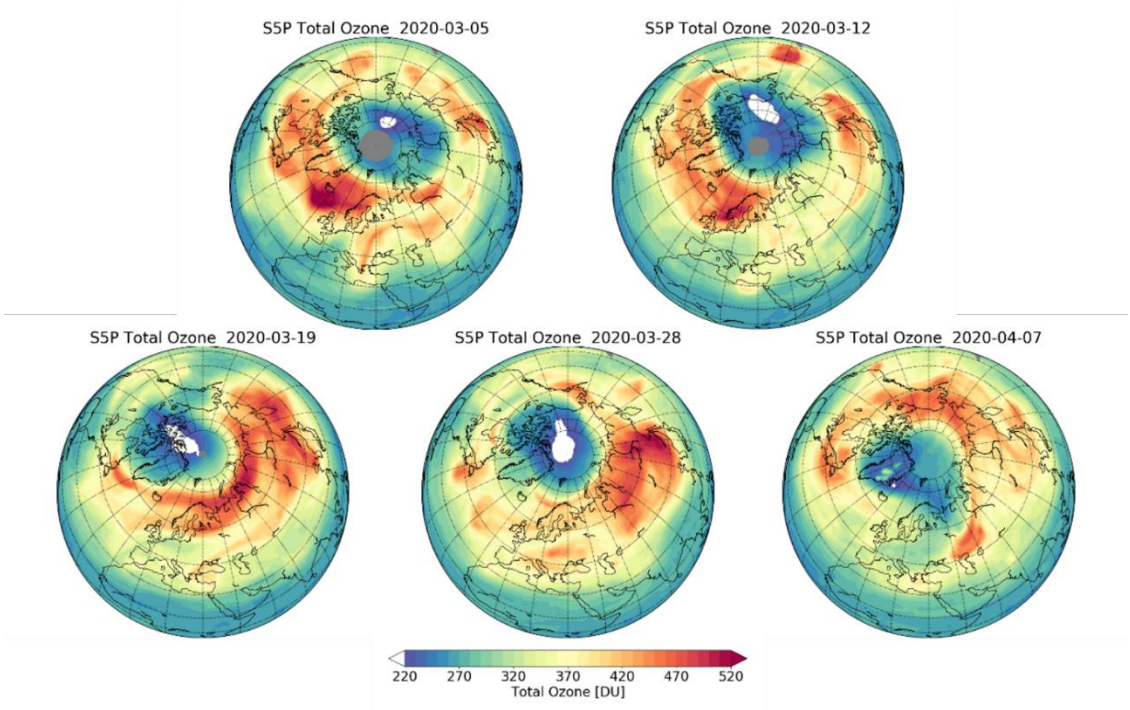

Figure 24: Total ozone column over the Northern Hemisphere on 5, 12, 19, and 28 March and 7 April 2020 measured by the TROPOMI instrument on board the Sentinel-5 Precursor (S5P) satellite. The color scale shows Dobson units (DU). The area with total ozone column values below 220 DU is denoted by the white color. Grey areas near the North Pole indicate missing data during polar night. Figure is taken from Dameris et al. (2021).

The special situation in spring 2020 is compared and discussed in context with two other Northern Hemisphere spring seasons, namely those in 1997 and 2011, which also displayed relatively low total ozone column values (**Figure 25**). However, during

these years, total ozone columns below 220 DU over several consecutive days were not observed in spring. The similarities and differences of the atmospheric conditions of these three events and possible explanations for the observed features are presented and discussed. It becomes apparent that the monthly mean of the minimum total ozone column value for March 2020 (221 DU) was clearly below the respective values found in March 1997 (267 DU) and 2011 (252 DU), which highlights the special evolution of the polar stratospheric ozone layer in the Northern Hemisphere in spring 2020. A comparison with a typical ozone hole over the Antarctic (e.g., in 2016) indicates that although the Arctic spring 2020 situation is remarkable, with total ozone column values around or below 220 DU observed over a considerable area (up to 0.9 million km^2), the Antarctic ozone hole shows total ozone columns typically below 150 DU over a much larger area (of the order of 20 million km^2). Furthermore, total ozone columns below 220 DU are typically observed over the Antarctic for about 4 months (**Figure 25**).

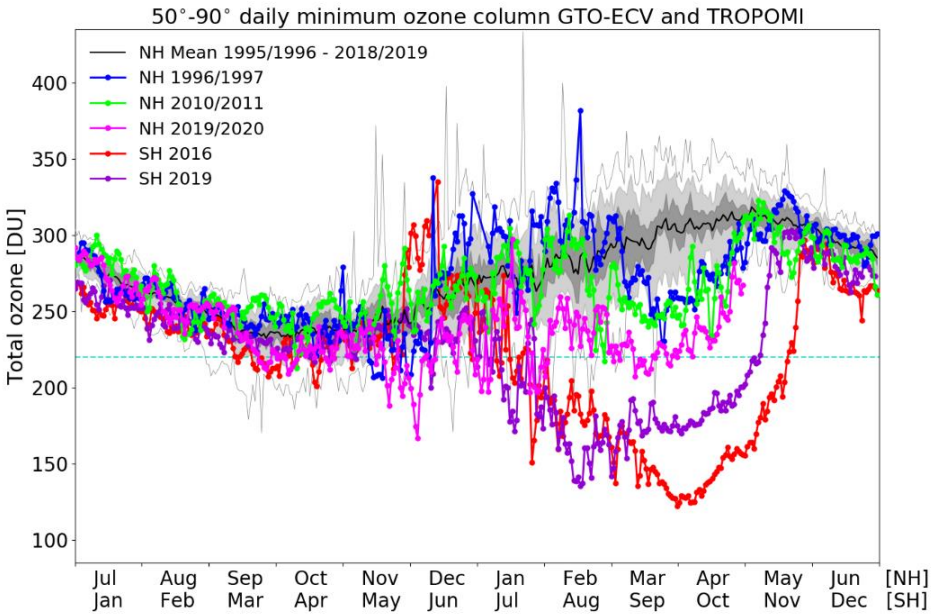

Figure 25: Annual cycle of the minimum total column ozone values (in Dobson Units, DU) in the north polar region between 50 and 90° N and in the south polar region between 50 and 90° S derived from the European satellite data record GOME-type Total Ozone Essential Climate Variable (GTO-ECV) from July 1995 to June 2019 and TROPOMI data from July 2019 to April 2020. The thick black line shows the GTO-ECV mean annual cycle in the north polar region, with the lowest ozone values in the fall season (October, November) and the highest ozone values in late spring (April, May). The thin black lines indicate the maximum and minimum values for the complete time period of satellite measurements starting in 1995. The light grey shading denotes the 10th percentile and the 90th percentile, and the dark grey shading denotes the 30th percentile and the 70th percentile, respectively. The magenta line shows the minimum values for the TROPOMI total ozone in the 2019/2020 season. The blue and green lines show the minimum values for the total ozone in the years 1996/1997 and 2010/2011, respectively. For comparison, the annual cycle of the minimum total column ozone values in the south polar region is shown in the years 2016 (red line) and 2019 (purple

line). The Southern Hemisphere data are shifted by 6 months. Figure is taken from Dameris et al. (2021).

4. Conclusions

Apart from the work performed within the Ozone_cci project, additional assessments have been carried out by the CCI - Climate Modelling User Group (CMUG). In particular, several Ozone_cci products were individually tested for assimilation in the ECMWF data assimilation system, using a configuration similar to the one that is employed for ERA5 (replacement of ERA-Interim). Among others, they found that the assimilation of these products could improve the meridional ozone gradients, and, by exploiting the synergy with other ozone products simultaneously assimilated, also improve the tropospheric ozone concentrations. A full account of the CMUG results to date can be found in the published CMUG Quality Assessment Report (version 0.5, 2015, http://ensembles-eu.metoffice.com/cmug/CMUG_D3.1_QAR_v0.5.pdf).

European research institutes and technological companies (business) could now expand the excellent starting position in areas of European research and technology. Moreover ESA-CCI fosters the dialogue and cooperation between climate observation and the modelling community. The interdependence of ECVs is another emerging topic for the near future. Are observed trends and changes consistent? Can one ECV be used to improve the observation of another?

Other important questions, which should be answered in near future, are how do we use in practice the new prolonged data sets of “Ozone_cci” and what do we learn from the data sets on the UT/LS and troposphere?

Looking ahead, ESA is in an excellent position to evaluate the quality of its space-borne observations, to reap benefits from new data products, including uncertainty measures and consequently to further develop and improve coming missions. European research institutes and organizations should be able to propose new and successful future space-borne missions.

Acknowledgement

Thanks to Massimo Valeri, University of Bologna, Italy, for preparing and analyzing the MIPAS ozone data and determining the differences regarding the EMAC model simulations.

References:

Adcock, K. E., P. J. Fraser, B. D. Hall, R. L. Langenfelds, G. Lee, S. A. Montzka et al., Aircraft-based observations of ozone-depleting substances in the upper troposphere and lower stratosphere in and above the Asian summer monsoon, J. Geophys. Res.-Atmos., 126, e2020JD033137, https://doi.org/10.1029/2020JD033137, 2021.

Albers, J.R., and T.R. Nathan, Pathways for communicating the effects of stratospheric ozone to the polar vortex: Role of zonally asymmetric ozone, J. Atmos. Sci., 69, 785-801, 2012.

Anstey, J. A., et al., Teleconnections of the Quasi-Biennial Oscillation in a multi-model ensemble of QBO-resolving models, Q. J. R. Meteorol. Soc., 1-25, doi: 10.1002/qj.4048, 2021.

Banerjee, A., J. C. Fyfe, L. M. Polvani, D. Waugh, and K.-L. Chang, A pause in Southern Hemisphere circulation trends due to the Montreal Protocol, Nature, 579, 544-548, https://doi.org/10.1038/s41586-020-2120-4, 2020.

Barnes, P.W., C. E. Williamson, R. M. Lucas, R.M. et al., Ozone depletion, ultraviolet radiation, climate change and prospects for a sustainable future, Nature Sustain., 2, 569-579, https://doi.org/10.1038/s41893-019-0314-2, 2019.

Bosilovich, M., Akella, S., Coy, L., Cullather, R., Draper, C., Gelaro, R., Kovach, R., Liu, Q., Molod, A., Norris, P., Wargan, K., Chao, W., Reichle, R., Takacs, L., Vikhliaev, Y., Bloom, S., Collow, A., Firth, S., Labow, G., Partyka, G., Pawson, S., Reale, O., Schubert, S. D., and Suarez, M., MERRA-2: Initial Evaluation of the Climate, Tech. rep., Series on Global Modeling and Data Assimilation, edited by: Koster, R. D., NASA Goddard Space Flight Center, Greenbelt, Maryland, NASA/TM-2015-104606, Vol. 43, 2015.

Calvo, N., R. R. Garcia, W. J. Randel, and D. R. Marsh, Dynamical mechanism for the increase in tropical upwelling in the lowermost tropical stratosphere during warm ENSO events, J. Atmos. Sci., 67, 2331-2340, doi: 10.1175/2010JAS3433.1, 2010.

Coldewey-Egbers, M., D. Loyola, P. Braesicke, M. Dameris, M. van Roozendael, C. Lerot, and W. Zimmer, A new health check of the ozone layer at global and regional scales, Geophys. Res. Lett., 41, 4363-4372, doi: 10.1002/2014GL060212, 2014.

Coldewey-Egbers, M., D. Loyola, M. Koukouli, D. Balis, J.-C. Lambert, T. Verhoelst, J. Granville, M. van Roozendael, C. Lerot, R. Spurr, S. M. Frith, and C. Zehner, The GOME-type Total Ozone Essential Climate Variable (GTO-ECV) data record from the ESA Climate Change Initiative, Atmos. Meas. Tech., 8, 3923-3940, doi: 10.5194/amt-8-3923-2015, 2015.

Coldewey-Egbers, M., Loyola, D. G., Labow, G., and Frith, S. M., Comparison of GTO-ECV and adjusted MERRA-2 total ozone columns from the last 2 decades and assessment of interannual variability, Atmos. Meas. Tech., 13, 1633–1654, https://doi.org/10.5194/amt-13-1633-2020, 2020.

Dameris, M., and D. Loyola, Chemistry-climate connections – Interaction of physical, dynamical, and chemical processes in Earth atmosphere, Chapter 1 in Climate Change - Geophysical Foundations and Ecological Effects (Open Access Book), Eds. J. Blanco and H. Kheradmand, Publisher: InTech, ISBN 978-953-307-419-1, pp. 3-24, 2011. Available from: http://www.intechopen.com/articles/show/title/chemistry-climate-connections-interaction-of-physical-dynamical-and-chemical-processes-in-earth-atmo

Dameris, M., P. Jöckel and M. Nützel, Possible implications of enhanced chlorofluorocarbon-11 concentrations on ozone, Atmos. Chem. Phys., 19, 13759–13771, https://doi.org/10.5194/acp-19-13759-2019, 2019.

Dameris, M., D. G. Loyola, M. Nützel, M. Coldewey-Egbers, C. Lerot, F. Romahn, and M. van Roozendael, Record low ozone values over the Arctic in boreal spring 2020, Atmos. Chem. Phys., 21, 617-633, https://doi.org/10.5194/acp-21-617-2021, 2021.

Dee, D. P., Uppala, S. M., Simmons, A. J., Berrisford, P., Poli, P., Kobayashi, S., Andrae, U., Balmaseda, M. A., Balsamo, G., Bauer, P., Bechtold, P., Beljaars, A. C. M., van de Berg, L., Bidlot, J., Bormann, N., Delsol, C., Dragani, R., Fuentes, M., Geer, A. J., Haimberger, L., Healy, S. B., Hersbach, H., Hólm, E. V., Isaksen, L., Kållberg, P., Köhler, M., Matricardi, M., McNally, A. P., Monge-Sanz, B. M., Morcrette, J.-J., Park, B.-K., Peubey, C., de Rosnay, P., Tavolato, C., Thépaut, J.-N. and Vitart, F., The ERA-Interim reanalysis: configuration and performance of the data assimilation system. Q. J. R. Meteorol. Soc., 137, 553-597. doi: 10.1002/qj.828, 2011.

Dhomse, S., D. Kinnison, M. P. Chipperfield, I. Cionni, M. Hegglin, N. L. Abraham, H. Akiyoshi, A. T. Archibald, E. M. Bednarz, S. Bekki, P. Braesicke, N. Butchart, M. Dameris, M. Deushi, S. Frith, S. C. Hardiman, B. Hassler, L. W. Horowitz, R.-M. Hu, P. Jöckel, B. Josse, O. Kirner, S. Kremser, U. Langematz, J. Lewis, M. Marchand, M. Lin, E. Mancini, V. Marécal, M. Michou, O. Morgenstern, F. M. O'Connor, L. Oman, G. Pitari, D. A. Plummer, J. A. Pyle, L. E. Revell, E. Rozanov, R. Schofield, A. Stenke, K. Stone, K. Sudo, S. Tilmes, D. Visioni, Y. Yamashita, G. Zeng, Estimates of ozone return dates from Chemistry-Climate Model Initiative simulations, Atmos. Chem. Phys., 18, 8409-8438, https://doi.org/10.5194/acp-18-8409-2018, 2018.

Dhomse, S., W. Feng, S. A. Montzka, R. Hossaini, J. Keeble, J. A. Pyle, J. S. Daniel, and M. P. Chipperfield, Delay in recovery of the Antarctic ozone hole from unexpected CFC-11 emissions, Nature Communications, 10, 5781, doi:10.1038/s41467-019-13717-x, 2019.

Döscher, R., Acosta, M., Alessandri, A., Anthoni, P., Arneth, A., Arsouze, T., Bergmann, T., Bernadello, R., Bousetta, S., Caron, L.-P., Carver, G., Castrillo, M., Catalano, F., Cvijanovic, I., Davini, P., Dekker, E., Doblas-Reyes, F. J., Docquier, D., Echevarria, P., Fladrich, U., Fuentes-Franco, R., Gröger, M., v.

Hardenberg, J., Hieronymus, J., Karami, M. P., Keskinen, J.-P., Koenigk, T., Makkonen, R., Massonnet, F., Ménégoz, M., Miller, P. A., Moreno-Chamarro, E., Nieradzik, L., van Noije, T., Nolan, P., O'Donnell, D., Ollinaho, P., van den Oord, G., Ortega, P., Prims, O. T., Ramos, A., Reerink, T., Rousset, C., Ruprich-Robert, Y., Le Sager, P., Schmith, T., Schrödner, R., Serva, F., Sicardi, V., Sloth Madsen, M., Smith, B., Tian, T., Tourigny, E., Uotila, P., Vancoppenolle, M., Wang, S., Wårlind, D., Willén, U., Wyser, K., Yang, S., Yepes-Arbós, X., and Zhang, Q.: The EC-Earth3 Earth System Model for the Climate Model Intercomparison Project 6, Geosci. Model Dev. Discuss. [preprint], https://doi.org/10.5194/gmd-2020-446, in review, 2021.

Fleming, E.L., P. A. Newman, Q. Liang, and J. S. Daniel, The impact of continuing CFC-11 emissions on stratospheric ozone, J. Geophys. Res., 125, e2019JD031849.doi.org:10.1029/2019JD031849, 2020.

Fortuin, J. P. F. and H. Kelder, An ozone climatology based on ozonesonde and satellite measurements, J. Geophys. Res., 103, D24, 31,709-31,734, 1998.

Frith, S. M., Kramarova, N. A., Stolarski, R. S., McPeters, R. D., Bhartia, P. K., and Labow, G. J., Recent changes in total column ozone based on the SBUV Version 8.6 Merged Ozone Data Set, J. Geophys. Res.-Atmos., 119, 9735–9751, https://doi.org/10.1002/2014JD021889, 2014.

Frith, S. M., Stolarski, R. S., Kramarova, N. A., and McPeters, R. D., Estimating uncertainties in the SBUV Version 8.6 merged profile ozone data set, Atmos. Chem. Phys., 17, 14695–14707, https://doi.org/10.5194/acp-17-14695-2017, 2017.

Hazeleger, W., X. Wang, C. Severijns, S. Stefanescu, R. Bintanja, A. Sterl, K. Wyser, T. Semmler, S. Yang, B. van den Hurk, T. van Noije, E. van der Linden, K. van der Wieland, EC-Earth V2: description and validation of a new seamless Earth system prediction model, Clim. Dyn., 39(11), 2611-2629, doi: 10.1007/s00382-011-1228-5, 2012.

Huijnen, V., Williams, J., van Weele, M., van Noije, T., Krol, M., Dentener, F., Segers, A., Houweling, S., Peters, W., de Laat, J., Boersma, F., Bergamaschi, P., van Velthoven, P., Le Sager, P., Eskes, H., Alkemade, F., Scheele, R., Nédélec, P., and Pätz, H.-W., The global chemistry transport model TM5: description and evaluation of the tropospheric chemistry version 3.0, Geosci. Model Dev., 3, 445-473, doi:10.5194/gmd-3-445-2010, 2010.

Huijnen, V., K. Miyazaki, J. Flemming, A. Inness, T. Sekiya, and M. G. Schultz, An intercomparison of tropospheric ozone reanalysis products from CAMS, CAMS interim, TCR-1, and TCR-2, Geosci. Model Dev., 13, 1513–1544, https://doi.org/10.5194/gmd-13-1513-2020, 2020.

Inness, A., M. Ades, A. Agustí-Panareda, J. Barré, A. Benedictow, A.-M. Blechschmidt, J. J. Dominguez, R. Engelen, H. Eskes, J. Flemming, V. Huijnen,

L. Jones, Z. Kipling, S. Massart, M. Parrington, V.-H. Peuch, M. Razinger, S. Remy, M. Schulz, and M. Suttie, The CAMS reanalysis of atmospheric composition, Atmos. Chem. Phys., 19, 3515–3556, https://doi.org/10.5194/acp-19-3515-2019, 2019.

Ivy, D. J., S. Solomon, N. Calvo, and D. W. J. Thompson, Observed connections of Arctic stratospheric ozone extremes to Northern Hemisphere surface climate, Environ. Res. Lett., 12, doi: 10.1088/1748-9326/aa57a4, 2017.

Jöckel, P., Tost, H., Pozzer, A., Kunze, M., Kirner, O., Brenninkmeijer, C. A. M., Brinkop, S., Cai, D. S., Dyroff, C., Eckstein, J., Frank, F., Garny, H., Gottschaldt, K.-D., Graf, P., Grewe, V., Kerkweg, A., Kern, B., Matthes, S., Mertens, M., Meul, S., Neumaier, M., Nützel, M., Oberländer-Hayn, S., Ruhnke, R., Runde, T., Sander, R., Scharffe, D., and Zahn, A., Earth System Chemistry integrated Modelling (ESCiMo) with the Modular Earth Submodel System (MESSy) version 2.51, Geosci. Model Dev., 9, 1153-1200, doi: 10.5194/gmd-9-1153-2016, 2016.

Keeble, J., et al., Modelling the potential impacts of the recent, unexpected increase in CFC-11 emissions on total column ozone recovery, Atmos. Chem. Phys., 20, 7153-7166, https://doi.org/10.5194/acp-20-7153-2020, 2020.

Keeble, J., et al., Evaluating stratospheric ozone and water vapour changes in CMIP6 models from 1850 to 2100, Atmos. Chem. Phys., 21, 5015-5061, https://doi.org/10.5194/acp-21-5015-2021, 2021.

Kunze, M., Braesicke, P., Langematz, U., and Stiller, G., Interannual variability of the boreal summer tropical UTLS in observations and CCMVal-2 simulations, Atmos. Chem. Phys., 16, 8695–8714, doi: 10.5194/acp-16-8695-2016, 2016.

Loyola R., D.G., M. Coldewey-Egbers, M. Dameris, H. Garny, A. Stenke, M. van Roozendael, C. Lerot, D. Balis, and M. Koukouli, Global long-term monitoring of the ozone layer - a prerequisite for predictions, Int. J. Remote Sensing, 30, Nos. 15-16, 4295-4318, doi: 10.1080/01431160902825016, 2009.

Maycock, A. C., W. J. Randel, A. K. Steiner, A. Y. Karpechko, J. Christy, R. Saunders, D. W. J. Thompson, C.-Z. Zou, A. Chrysanthou, N. L. Abraham, H. Akiyoshi, A. T. Archibald, N. Butchart, M. Chipperfield, M. Dameris, M. Deushi, S. Dhomse, G. Di Genova, P. Jöckel, D. E. Kinnison, O. Kirner, F. Ladstaedter, M. Michou, O. Morgenstern, F. O´Connor, L. Oman, G. Pitari, D. A. Plummer, L. E. Revell, E. Rozanov, A. Stenke, D. Visioni, Y. Yamashita, and G. Zeng, Revisiting the mystery of recent stratospheric temperature trends, Geophys. Res. Lett., 45, 9919-9933, https://doi.org/10.1029/2018GL078035, 2018.

McCormack, J.P., T.R. Nathan, and E.C. Cordero, The effect of zonally asymmetric ozone heating on the Northern Hemisphere winter polar stratosphere, Geophys. Res. Lett., 38, L03802, 2011.

Meul, S., M. Dameris, U. Langematz, J. Abalichin, A. Kerschbaumer, A. Kubin, and S. Oberländer-Hayn, Impact of rising greenhouse gas concentrations on future tropical ozone and UV exposure, Geophys. Res. Lett., 43, 2919-2927, doi: 10.1002/2016GL067997, 2016.

Montzka, S. A. et al., An unexpected and persistent increase in emissions of ozone-depleting CFC-11, Nature, 557, 413-417, 2018.

Montzka, S. A., G. S. Dutton, R. W. Portmann, et al., A decline in global CFC-11 emissions during 2018-2019, Nature, 590, 428-432, https://doi.org/10.1038/s41586-021-03260-5, 2021.

Morgenstern, O., M. I. Hegglin, E. Rozanov, F. M. O'Connor, et al., Review of the global models used within phase 1 of the Chemistry–Climate Model Initiative (CCMI), Geosci. Model Dev., 10, 639-671, doi:10.5194/gmd-10-639-2017, 2017.

Noije, T. P. C., P. Le Sager, A. J. Segers, P. F. J. van Velthoven, M. C. Krol, and W. Hazeleger, Simulation of tropospheric chemistry and aerosols with the climate model EC-Earth, Geosci. Model Dev. Discuss., 7, 1933–2006, 2014.

Noije, T. P. C., T. Bergman, P. Le Sager, D. O'Donnell, R. Makkonen, M. Gonçalves-Ageitos, R. Döscher, U. Fladrich, J. von Hardenberg, J.-P. Keskinen, H. Korhonen, A. Laakso, S. Myriokefalitakis, P. Ollinaho, C. Pérez García-Pando, T. Reerink, R. Schrödner, K. Wyser, and S. Yang, EC-Earth3-AerChem, a global climate model with interactive aerosols and atmospheric chemistry participating in CMIP6, Geosci. Model Dev. Discuss., https://doi.org/10.5194/gmd-2020-413, 2020.

Ravishankara, A. R., J. S. Daniel, R. W. Portmann, Nitrous oxide (N_2O): The dominant ozone-depleting substance emitted in the 21st century, Science, 326, 123–125, 2009.

Rigby, M., S. Park, T. Saito, et al., Increase in CFC-11 emissions from eastern China based on atmospheric observations, Nature 569, 546-550, https://doi.org/10.1038/s41586-019-1193-4, 2019.

Solomon, S., et al., Emergence of healing in the Antarctic ozone layer, Science, doi: 10.1126/science.aae0061, 2016.

SPARC/IO3C/GAW, Report on Long-term Ozone Trends and Uncertainties in the Stratosphere. I. Petropavlovskikh, S. Godin-Beekmann, D. Hubert, R. Damadeo, B. Hassler, V. Sofieva (Eds.), SPARC Report No. 9, GAW Report No. 241, WCRP-17/2018, doi: 10.17874/f899e57a20b, available at www.sparc-climate.org/publications/sparc-reports, 2019.

Tarasick, D., Galbally, I. E., Cooper, O. R., Schultz, M. G., Ancellet, G., Leblanc, T., Wallington, T. J., Ziemke, J., Liu, X., Steinbacher, M., Staehelin, J., Vigouroux, C., Hannigan, J. W., García, O., Foret, G., Zanis, P., Weatherhead, E., Petropavlovskikh, I., Worden, H., Osman, M., Liu, J., Chang, K.-L., Gaudel, A., Lin, M., Granados-Muñoz, M., Thompson, A. M., Oltmans, S.J., Cuesta, J.,

Dufour, G., Thouret, V., Hassler, B., Trickl, T. and Neu, J.L., Tropospheric Ozone Assessment Report: Tropospheric ozone from 1877 to 2016, observed levels, trends and uncertainties, Elem. Sci. Anth., 7(1), p.39, doi: 10.1525/elementa.376, 2019.

Thompson, D., Solomon, S., Kushner, P., et al., Signatures of the Antarctic ozone hole in Southern Hemisphere surface climate change, Nature Geosci., 4**,** 741-749, https://doi.org/10.1038/ngeo1296, 2011.

Vyushin, D., V.E. Fioletov, and T.G. Shepherd, Impact of long-range correlations on trend detection in total ozone, J. Geophys. Res., 112, D14307, doi: 10.1029/2006JD008168, 2007.

Weatherhead, E.C., et al., Factors affecting the detection of trends: Statistical considerations and applications to environmental data, J. Geophys. Res., 103(D14), 17149-17161, doi: 10.1029/98JD00995, 1998.

WMO (World Meteorological Organization), Scientific Assessment of Ozone Depletion: 2006, Global Ozone Research and Monitoring Project, Report No. 50, 572 pp. (ISBN 978-92-807-2756-2), Geneva, Switzerland, 2007.

WMO (World Meteorological Organization), Scientific Assessment of Ozone Depletion: 2010, Global Ozone Research and Monitoring Project, Report No. 52, 516 pp. (ISBN: 9966-7319-6-2), Geneva, Switzerland, 2011.

WMO (World Meteorological Organization), Scientific Assessment of Ozone Depletion: 2014, Global Ozone Research and Monitoring Project, Report No. 55, 416 pp. (ISBN: 978-9966-076-01-4), Geneva, Switzerland, 2014.

WMO (World Meteorological Organization), Scientific Assessment of Ozone Depletion: 2014, Global Ozone Research and Monitoring Project, Report No. 58, 588 pp. (ISBN: 978-1-7329317-1-8), Geneva, Switzerland, 2018.

WMO (World Meteorological Organization), Report on the unexpected emissions of CFC-11, WMO-No. 1268, 88 pp. (ISBN 978-92-63-11268-2), Geneva, Switzerland, 2021.

Yarwood, G., Rao, S., Yocke, M., and Whitten, G.: Updates to the carbon bond chemical mechanism: CB05, Final report to the US EPA, EPA Report Number: RT-0400675, available at: http://www.camx.com (last access: 15 March 2019), 2005.